01 Dec 1978

Deck-reinforced slab systems

Max L. Porter

C. E. Ekberg Jr.

This bulletin is another in the series of engineering research bulletins published by the Engineering Research Institute, Iowa State University. Please address all correspondence to: Editor, Engineering Research Institute, 104 Marston Hall, Iowa State University, Ames, Iowa 50011

ENGINEERING RESEARCH
ENGINEERING RESEARCH
ENGINEERING RESEARCH
ENGINEERING RESEARCH
ENGINEERING RESEARCH

BULLETIN 200

COMPENDIUM OF ISU RESEARCH CONDUCTED ON COLD-FORMED STEEL-DECK-REINFORCED SLAB SYSTEMS

M. L. Porter
C. E. Ekberg, Jr.
December 1978

Price: $10.00

ISU-ERI-AMES-78263
ENGINEERING RESEARCH INSTITUTE
IOWA STATE UNIVERSITY AMES

COMPENDIUM OF ISU RESEARCH CONDUCTED ON COLD-FORMED STEEL-DECK-REINFORCED SLAB SYSTEMS

ABSTRACT

An extensive theoretical and experimental research program on steel-deck-reinforced floor systems has been conducted at Iowa State University. A total of 353 full-scale tests were performed on the following types of specimens: pushout, single span slab elements with steel deck corrugations oriented parallel to span length, slab elements with steel deck corrugations oriented transverse to span length, slab elements continuous over two or three spans, slab elements subjected to repeated loading, slab elements constructed with variable supplementary reinforcement, slab elements constructed with noncomposite deck having various surface coatings, full-size two-way floor slabs simply supported on four edges, slab elements with various shoring conditions, and slab elements subjected to uniform versus concentrated loading. The purpose of the above tests was to investigate typical behavioral characteristics and modes of failure. The principal failure mode was found to be that of shear-bond, for which design equations were formulated to predict the capacity. The primary objective of the research program was to develop information leading to specifications governing the application, use, and design of concrete slabs reinforced with cold-formed steel decking.

TABLE OF CONTENTS

	Page
ABSTRACT	iii
LIST OF TABLES	vii
LIST OF FIGURES	ix
NOTATION	xi
ACKNOWLEDGMENTS	xv
1. INTRODUCTION	1
2. DESCRIPTION OF RESEARCH PROGRAM	5
2.1. Tests	5
2.2. Test Data, Primary Parameters and Notation	5
2.3. Reports and Publications	9
3. PUSHOUT TESTS	11
4. ONE-WAY SLAB ELEMENT TESTS	15
4.1. General	15
4.2. Description of Failure Modes	15
4.2.1. Shear-Bond	16
4.2.2. Flexure	19
5. DETERMINATION OF SHEAR-BOND STRENGTH	21
5.1. Strength Prediction Equations	22
5.2. Example Shear-Bond Formulations	24
5.3. Comparison of Theoretical and Experimental Results	33
6. DETERMINATION OF FLEXURAL STRENGTH	39
6.1. Conventional Methods	39
6.2. General Strain Analysis	40
7. DEFLECTION BEHAVIOR	45

		Page
8.	REPEATED LOAD TESTS	47
9.	CONTINUOUS SPANS	49
10.	FULL-SCALE TWO-WAY SLABS	53
	10.1. Description	53
	10.2. Test Results	53
11.	ELEMENTS WITH TRANSVERSE CORRUGATIONS	65
12.	EFFECTS OF VARIOUS SURFACE COATINGS	67
13.	UNIFORM LOAD TESTS	69
14.	SLAB ELEMENTS WITH VARIOUS SHORING CONDITIONS	71
15.	SLAB ELEMENTS WITH VARIABLE AMOUNTS OF SUPPLEMENTARY REINFORCEMENT	73
16.	SUMMARY	75
17.	REFERENCES	77
18.	APPENDIX: COMPLETE LIST OF PUBLISHED PAPERS AND THESES RELATING TO ISU RESEARCH	79

LIST OF TABLES

		Page
1.	Categories of tests conducted	6
2.	Variable identification for one-way slab element data	7
3.	Possible equations for shear-bond failure	24
4.	Common variables for linear regression groups	26
5.	Results of linear regression analyses showing average percent errors and correlation coefficients	27
6.	Summary of significant material properties for two-way slab specimens	55
7.	Load results for five full-scale slab tests	56
8.	Experimental effects of elements containing WWF	73

LIST OF FIGURES

		Page
1.	Typical building floor construction utilizing cold-formed steel decking with composite support beams	1
2.	Examples of composite steel-deck floor slab systems	2
3.	Illustration of a typical cellular and noncellular type of deck profile	3
4.	Vertical pushout specimens	11
5.	Example of embedment length vs total mechanical bond and effective stress for pushout tests	12
6.	Typical arrangement for testing one-way slab elements	15
7.	Typical shear-bond failure	16
8.	Photograph of end-slip after failure of a one-way slab element	17
9.	Typical shear-bond failures of one-way slab elements of various shear span lengths	18
10.	Typical load-displacement relationships for end-slip	19
11.	View showing flexural failure of under-reinforced slab element	20
12.	Typical shear-bond plot showing the reduced evaluation of m and k	22
13.	Example plots illustrating the effect of gage thickness for Equation B utilizing Deck 1	29
14.	Example regression plots for Equation B utilizing Decks 2 and 3	30
15.	Example regression plots for Equation B utilizing Decks 4 and 5	31
16.	Example regression plot for Equation B utilizing Deck 6	32
17.	Example load-deflection relationships of various shear spans and span lengths showing the allowable live load for specimens reinforced with 18 gage steel deck	35
18.	Example load-deflection relationships showing the effects of specimens reinforced with different gage thicknesses of steel deck	36

		Page
19.	Linear regression relationships for obtaining design live loads indicated in Figs. 17 and 18	37
20.	Strain-compatibility diagrams for general flexural strain analysis	42
21.	Example of experimental vs theoretical load-deflection behavior	45
22.	Load vs centerline deflection of various continuous beams	50
23.	Diagram showing how uniformly loaded continuous beam may be subdivided into a series of simple spans for analysis	51
24.	General configuration and support conditions for full-scale slab tests	53
25.	Crack patterns on top surface of each slab	58
26.	View showing Slab 4 with diagonal edge cracking accompanied by end-slip	59
27.	Collapse mechanism and effective load-carrying segment used for analysis of five full-scale slabs	60
28.	Load vs centerpoint deflection for entire final load cycle	61
29.	Distribution of reactive forces along the south and west supports for Slabs 1, 2, 3, and 5	62
30.	Percentage of applied load transmitted to each reaction support as loading increases for Slabs 1, 2, 3, and 5	63
31.	Typical test on slab element with transverse decking	65
32.	Plot of shear-bond strength of slab elements containing WWF compared to those without WWF	74

NOTATION

Symbol	Definition
A_s	Cross-sectional area of steel deck or negative moment reinforcing steel where used as tension reinforcement, $in.^2/ft$ of width
a	Depth of equivalent rectangular stress block, $(A_s F_y)/(0.85f'_c b)$, in.
b	Unit width of slab = 12 in.
b_b	Width of composite test slab, ft
C	Compressive force on cross section due to flexure, kips
C_m	Moment coefficient--depends on whether the slab is simply supported or continuous and on the distribution of loading
c.g.s.	Centroidal axis of full cross section of steel deck
D	Nominal out-to-out depth of slab, in.
D_{AVG}	Average measured out-to-out depth of depth of slab, in.
D_{cr}	Out-to-out depth of slab at failure crack in test specimen, in.
d	Effective slab depth (distance from extreme concrete compression fiber to centroidal axis of the full cross section of the steel deck), in.
d_d	Overall depth of steel deck profile, in.
$d_{y.x}$	Deviation of a particular test specimen data point from shear-bond regression line
DL_c	Concrete dead load, psf
DL_d	Steel deck dead load, psf
E	Earthquake load perpendicular to slab
E_c	Modulus of elasticity of concrete, psi (See ACI Building Code Section 8.5.1. [7]).
E_s	Modulus of elasticity of steel deck, 29,500,000 psi

F_u	Ultimate tensile strength of steel, psi
F_y	Specified yield point or yield strength of steel, psi
F_{yt}	Measured yield point or strength of steel, psi
f'_c	Specified compressive strength of concrete, psi
f'_{ct}	Compressive test cylinder strength at time of slab testing, psi
f_r	Modulus of rupture strength of concrete, psi
I_c	Moment of inertia of composite section based on cracked section, $in.^4/ft$ of width
I_u	Moment of inertia of composite section based on uncracked section, $in.^4/ft$ of width
I_{sf}	Moment of inertia of steel deck per foot of width based on full cross-sectional deck area, $in.^4/ft$ of width
k	Ordinate intercept of reduced shear-bond regression line (see Fig. 12)
k_1	Ordinate intercept of shear-bond regression line based upon experimental tests (see Fig. 12)
M_u	Ultimate calculated moment capacity based on flexural failure, ft-lb/ft of width
m	Reduced slope of reduced shear-bond regression line (see Fig. 12)
m_1	Slope of shear-bond regression line based upon experimental tests (see Fig. 12)
L	Length of span, ft
L'	Length of shear span, in.; for uniform load, L' = one quarter of the span
L''	Distance between inflection points in any particular span of a continuous slab, ft, or effective width distance of two-way slab
LL	Allowable superimposed live load for service conditions, psf
N.A.	Neutral axis of transformed composite section
n	The modular ratio, E_s/E_c

n	Total number of tests
P_e	Maximum applied experimental slab load at failure obtained from laboratory tests, lbs (includes weight of loading system but not weight of slab)
r	Coefficient of correlation for shear-bond regression
s	Center-to-center spacing of shear transfer devices, in.
T_B	Tensile force located at center of bottom horizontal elements of steel decking in general strain analysis, kips
T_T	Tensile force located at center of top horizontal elements of steel decking in general strain analysis, kips
T_W	Tensile force located at mid-depth of web elements of steel decking in general strain analysis, kips
t_c	Depth of concrete above steel deck, in.
t_d	Steel thickness exclusive of coating, in.
V_e	Maximum experimental shear at failure obtained from laboratory tests, lb/ft of width (not including weight of slab)
V_u	Calculated ultimate shear capacity based on shear-bond failure, lb/ft of width
W_1	Weight of slab ($DL_d + DL_c$), psf
W_3	Dead load applied to slab, exclusive of W_1, psf
X	Abscissa value for shear-bond regression (see Fig. 12) $= \frac{\rho d}{L'\sqrt{f'_{ct}}} = \frac{A_s}{12L'\sqrt{f'_{ct}}}$
Y	Ordinate value for shear-bond regression (see Fig. 12) $= \frac{V_e s}{12\ d\sqrt{f'_{ct}}}$
y_o	Distance from composite section neutral axis to compression force, C, in.
y_{sb}	Distance from centroidal axis of steel deck to bottom of steel deck, in.

β_1	Equals 0.85 for concrete with $f'_c \leq 4000$ psi, and is reduced at a rate of 0.05 for each 1000 psi of strength above 4000 psi, but β_1 shall not be taken less than 0.65
Δ	Midspan deflection, in.
γ	Coefficient for proportion of dead load added upon removal of shore
ε_{B_1}, ε_{B_2}, ε_{B_3}, ε_{B_4}	Strain in bottom fiber of steel decking for general strain analysis, microinches/in.
ε_{C_1}, ε_{C_2}, ε_{C_3}, ε_{C_4}	Strain at top fiber of concrete for general strain analysis, microinches/in.
ε_{T_1}, ε_{T_2}, ε_{T_3}, ε_{T_4}	Strain in top fiber of steel decking for general strain analysis, microinches/in.
ε_u	Maximum concrete compression strain at ultimate strength, in./in.
ε_{w_1}, ε_{w_2}, ε_{w_3}, ε_{w_4}	Strain in web sections of steel decking taken at mid-depth of web elements of steel deck for general strain analysis, microinches/in.
ϕ	Capacity reduction factor
ρ	Reinforcement ratio of steel deck area to concrete area, A_s/bd
ρ_b	Reinforcement ratio producing balanced conditions

ACKNOWLEDGMENTS

The research described in this bulletin was conducted under the auspices of the Engineering Research Institute of Iowa State University through funds provided by the American Iron and Steel Institute (AISI).

Valuable guidance was provided by the AISI's Task Committee on Composite Construction under the leadership of T. J. McCabe, Chairman, and A. J. Oudheusden, past Chairman. The Task Committee is attached to a Joint Engineering Subcommittee of the Committees of Hot Rolled and Cold Rolled Sheet and Strip Producers and Galvanized Sheet Producers. At this stage, the American Society of Civil Engineer's Technical Council on Codes and Standards Committee on Composite Steel Deck Slabs is utilizing pertinent information gained from this investigation to develop recommendations for the design of steel-deck-reinforced slabs.

The authors wish to acknowledge the contributions to the project of R. M. Schuster and other faculty colleagues and staff. Dr. Schuster's early efforts in developing a shear-bond analysis for steel-deck-reinforced slab systems was particularly important. A formidable statistical analysis of test data could not have been accomplished without the participation of Dr. L. F. Greimann and the late Dr. H. A. Elleby. A unique experimental investigation was conducted by Dr. F. W. Klaiber with the objective of ascertaining behavioral characteristics of slab elements under uniform loading. A useful test program on slab elements with steel deck having various surface conditions was conducted by J. C. Mauser in partial fulfillment of the requirements for his Master of Science degree. The work of L. A. Boettcher, who served on the project for five years as a laboratory assistant, and later as a research assistant, is greatly appreciated. Data compilation by L. W. Timm, graduate student, and laboratory aid by P. E. Manz should be mentioned along with over 100 students employed during the course of the investigation.

1. INTRODUCTION

An extensive theoretical and experimental investigation on various aspects of cold-formed steel decking as reinforcement for concrete floor slabs was initiated at Iowa State University (ISU) in 1967 by the Engineering Research Institute (ERI) under the sponsorship of the American Iron and Steel Institute (AISI). Direct guidance for the investigation was provided from AISI by their Task Group on Composite Construction. A description of the various phases of the research program including pertinent behavioral characteristics and modes of failure from test results is presented herein.

Cold-formed steel deck sections are used in many composite floor slab applications where the steel deck serves not only as the form for the concrete during construction, but also as the principal tensile reinforcement for the bottom fibers of the composite slab. The term "composite steel-deck floor slab" is applied to systems in which the steel deck has some mechanical means of providing positive interlocking between the deck and the concrete. An example is shown in Fig. 1.

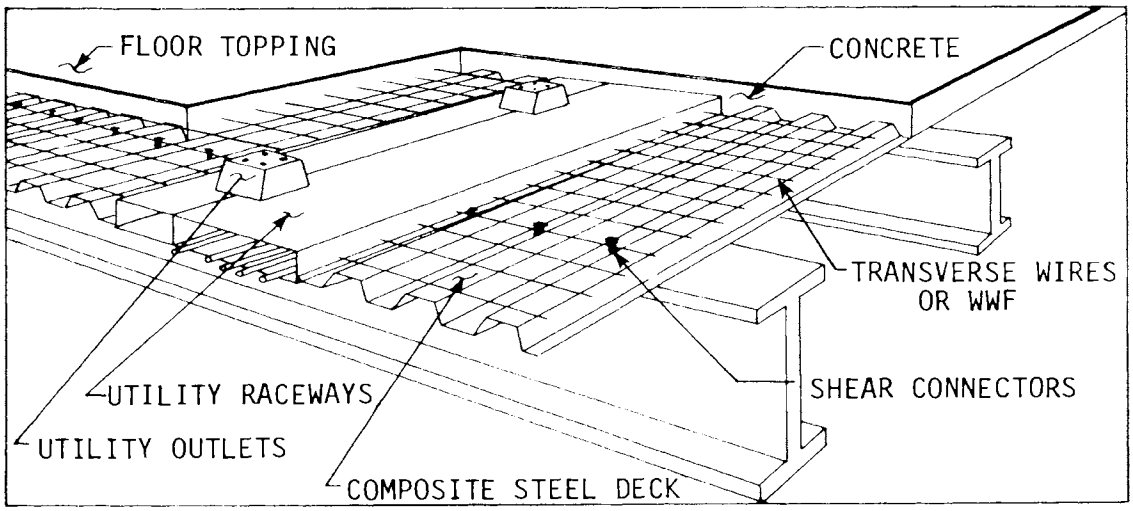

Fig. 1. Typical building floor construction utilizing cold-formed steel decking with composite support beams.

The mechanical means of positive interlocking between the deck and the concrete is usually achieved by one of the following:

1. Embossments and/or indentations,
2. Transverse wires attached to the deck corrugations,
3. Holes placed in the corrugations, and
4. Deck profile and steel surface bonding.

Figure 2 gives examples of composite steel decks which utilize each of

the above-listed means of composite interlocking. The mechanical interlocking and/or deck profile must provide for resistance to vertical separation and to horizontal slippage between the contact surface of the steel and concrete. Additional composite action may be achieved between the composite steel deck floor slab and the support beams by attaching studs or similar shear devices (see Fig. 1).

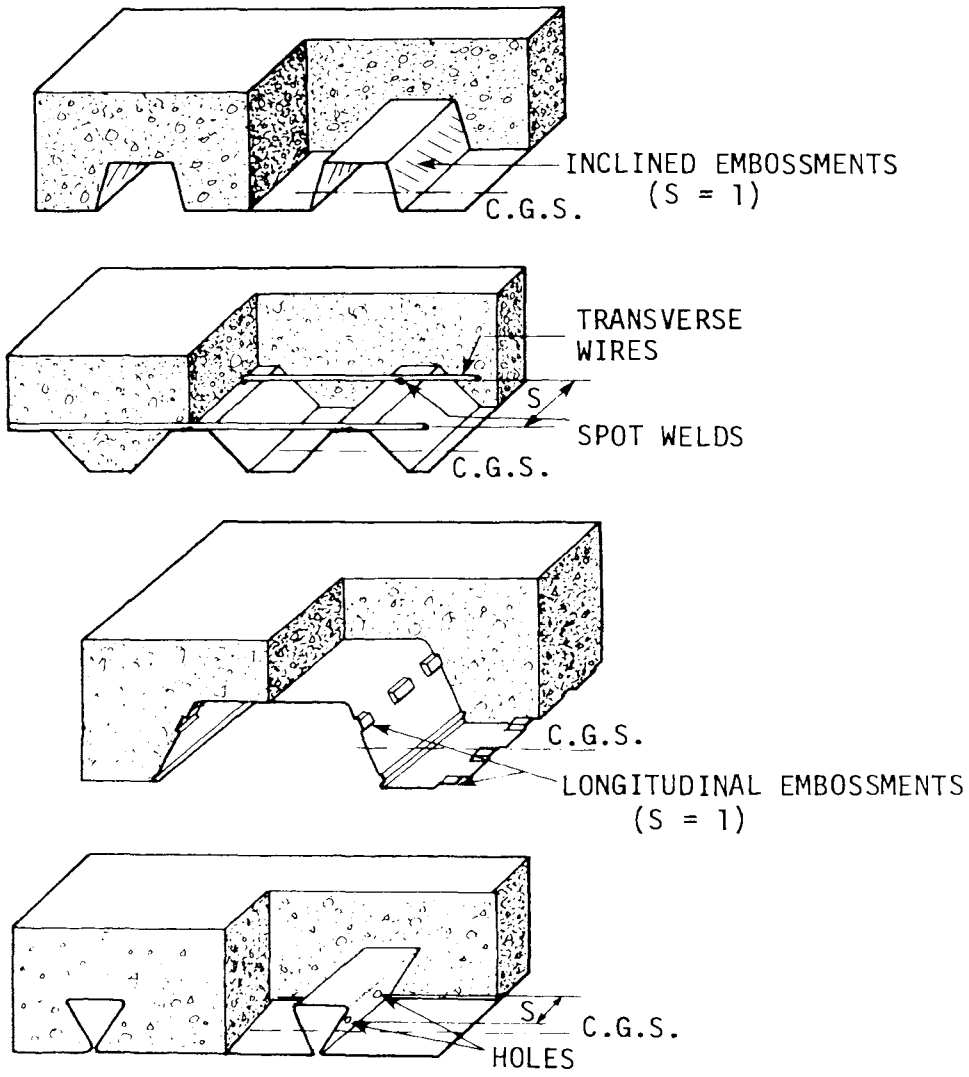

Fig. 2. Examples of composite steel-deck floor slab systems.

Steel deck profiles generally are classified as two types, namely cellular and noncellular (see Fig. 3). Cellular decks differ from noncellular ones in that the cellular deck profile has closed cells formed by an added sheet of steel connected to the bottom corrugations. The closed cells are often used for electrical, communication, or other utility raceways within the floor system. In some instances, utility raceways are blended with the composite deck profiles (see Fig. 1).

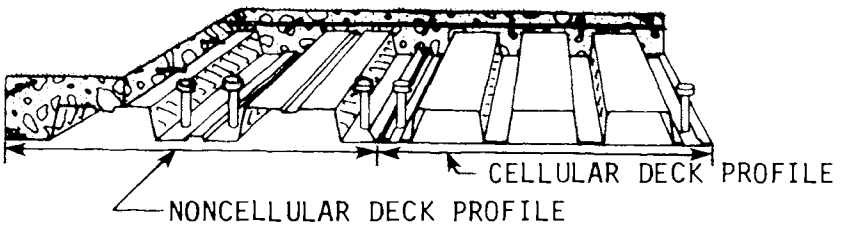

Fig. 3. Illustration of a typical cellular and noncellular type of deck profile.

The more important advantages of using cold-formed steel decking as reinforcement for a floor slab system can be summarized by the following statements.

1. The steel deck eliminates the need for installing much of the formwork which is usually necessary in concrete construction.

2. The stay-in-place feature of the deck saves a considerable amount of labor.

3. The composite deck serves as reinforcement for the floor slab, and only additional shrinkage, temperature, and negative moment reinforcement is needed.

4. The deck provides a ceiling surface, or in the case of a suspended ceiling, provides easy attachment of support hangers.

5. The deck can be easily placed and handled.

6. The corrugations of the deck contain pre-engineered ducting for electrification, communication, and air distribution.

7. The deck is palletized floor-by-floor for easy shipment and handling and reduces requirements for storage spaces.

8. After placement of the deck panels, the deck surface acts as a safe platform for the workmen, their tools, materials and equipment.

9. The likelihood of construction fires is greatly reduced since most combustible wooden formwork is removed.

10. Time of construction is greatly reduced since casting of additional floors may proceed without waiting for previously cast floors to gain strength to support shoring.

11. The use of steel decking reduces the dead load of the floor slab with little or no corresponding loss in load-carrying capacity.

2. DESCRIPTION OF RESEARCH PROGRAM

2.1. Tests

The major portion of the ISU research involved the testing to ultimate load of 353 full-scale specimens of various types. As can be seen in Table 1, the majority of the tests were conducted on one-way steel-deck-reinforced slab elements with their corrugations oriented parallel to the specimen length. Steel deck sections from five different manufacturers were utilized in the test program. A significant portion of the research effort was devoted to the study of the behavior of five full-size floor slabs under concentrated loading, such as that from a fork lift truck.

2.2. Test Data, Primary Parameters and Notation

The results from the various categories of the 353 tests, indicated in Table 1, were utilized for development of strength predictions and design recommendations. In addition, 151 one-way slab element tests, as reported by various manufacturers, were used in the research program.

The available data on one-way slab elements, from a total of 455 tests, embraces 304 tests from Table 1, plus 151 tests reported by various deck manufacturers. The primary test parameters included the following: manufacturer and deck type, nominal gage thickness of steel deck, shear span, an indication of a retested specimen, concrete pour number, age of testing, an indication of the presence of strain gages, ultimate applied load, dead load, type of failure, clear span length, center-to-center of bearings, type of loading, specimen width, average out-to-out depth, out-to-out depth at major failure crack, cross-sectional area of steel deck, distance between centroid of steel deck area and bottom of deck, depth of steel deck, steel deck thickness, moment of inertia of steel deck, yield strength and modulus of elasticity of steel deck, surface coating condition of deck, concrete compressive strength, shoring condition, presence of any supplementary reinforcing, spacing of mechanical shear transferring devices if a variable, an indication if the decks were greased, and type of concrete (lightweight or normal).

Table 2 contains a complete listing of the above variables as tabulated by a computer listing of all data given in [1] and [2].*

*Numbers in brackets denote references in section 17.

Table 1. Categories of tests conducted.

Item number	Number tested	Type of specimen[a] tested
1	56	Pushout specimens
2	178	One-way slab elements (beams)
3	14	One-way slab elements subjected to repeated loading
4	5	Slab elements continuous over two or three spans
5	5	Full-size two-way floor slabs simply supported on four edges
6	12	Slab elements with deck corrugations transverse to beam length
7	6	Slab elements constructed with variable supplementary reinforcement in the form of welded wire fabric
8	31	Slab elements constructed with 3 in. deep steel deck
9	34	Slab elements constructed with noncomposite deck with various surface coatings
10	6	Slab elements subjected to uniform versus concentrated loading
11	6	Slab elements with various shoring conditions
TOTAL	353	

[a]All tests on slab elements were conducted with specimens simply supported on a single span with static concentrated loads. Steel decking of 1.5 in. depth was used with corrugations oriented parallel to length unless otherwise indicated. All specimens were tested with noncellular type of steel decking.

Table 2. Variable identification for one-way slab element data (see [1] and [2]).

Variable No.	Description of variable	Code identification No. (if one exists)	Description of code identification number, or special notes
1	Manufacturer and deck type	100	First number indicates each manufacturer's deck followed by a pair of numbers indicating the particular deck type.
		200, 210, 220	
		300, 310, 320, 340, 350, 360, 370, 380, 390, 311	
		400, 410, 420, 430, 440, 450	
		500	
		600, 610, 620, 630	
2	Nominal gage thickness of steel deck	20	Number designates nominal gage thickness of deck unless a plate (for cellular deck) is attached under the decking, in which case the following designations are used:
		88	deck = 18 gage, plate = 18 gage
		86	deck = 18 gage, plate = 16 gage
		66	deck = 16 gage, plate = 16 gage
		64	deck = 16 gage, plate = 14 gage
		43	deck = 14 gage, plate = 13 gage
3	Shear span length, L', in inches	-	Taken as 1/4 times the span length for uniformly loaded specimens.
4	Original or retested specimen	0	Original test to failure. Retest of failure portion of specimen.
		1	
5	Concrete pour number	-	A zero pour number was used for the various manufacturer's test specimens.
6	Age at testing in days	-	------
7	Existence of strain gages on specimen	0	Specimen did not contain strain gages.
		1	Specimen did contain strain gages.
8	Total ultimate applied load, P_e, in kips	-	Does not include specimen dead weight, but does include loading apparatus.
9	Specimen dead weight, W_1, in pounds per square foot	-	Taken as an average uniform weight.
10	Type of failure	0	Shear-bond.
		1	Flexure by crushing of concrete.
		2	Flexure by rupture of steel deck.
11	Clear span length, L, in inches	-	------
12	Type of loading	0	Simple span subjected to two concentrated loads located at a distance L' from end support, except when L' = L/2 when only one concentrated load existed.
		1	Simple span subjected to uniform loading.
		5	Low-cycle repeated load application consisting of 3 to 6 cycles.
13	Specimen width, b_b, in inches	-	------
14	Average out-to-out depth of specimen, D_{avg}, in inches	-	------
15	Out-to-out depth at failure crack, D_{cr}, in inches	-	This depth applied to those specimens failing by the shear-bond mode.

(Continued)

Table 2. Continued.

Variable No.	Description of variable	Code identification No. (if one exists)	Description of code identification number, or special notes
16	Area of steel deck, A_g, in square inches per foot of width	-	------
17	Distance from bottom fiber of steel deck to the centroid of the deck, y_{sb}, in inches	-	------
18	Depth of steel deck, d_d, in inches	-	------
19	Steel deck thickness, t_d, in inches	-	------
20	Moment of inertia of steel deck, I_{sf}, in inches to fourth per foot of width	-	Calculated based on full deck cross-section unless measurements not available, in which case catalog values were used.
21	Yield strength of steel deck, F_{yt}, in kips per square inch	-	A zero indicates that F_{yt} data was not taken. An estimated F_{yt} of 40 ksi would probably suffice if the yield strength is desired.
22	Modulus of elasticity of steel deck, E_s, in 10^3 kips per square inch	-	If a measured value of E_s was unavailable, then E_s was assumed equal to 29,500 ksi.
23	Surface coating condition	1	Wiped coating on embossed deck.
		2	Wiped coating on non-embossed deck.
		3	Enameled coating on embossed deck.
		4	Enameled coating on non-embossed deck.
		5	Galvanized nominal one-half ounce per square foot on either embossed or non-embossed.
		6	Galvanized nominal 1.25 oz per square foot on embossed deck.
		7	Galvanized nominal one-and-one-quarter ounces per square foot on non-embossed deck.
		8	Plain steel deck with no added coating on non-embossed or embossed deck.
		9	Rusted plain steel on non-embossed deck.
		0	Vinsynite primer on embossed deck.
24	Concrete compressive strength, f'_{ct}, in pounds per square inch	-	------
25	Type of shoring condition used during casting of specimens	1	Specimen was supported at each end and center.
		2	Specimen was continuously supported.
		3	Specimen was supported at each end only.
		5	Specimen supported at one foot from each end.
		6	Specimen supported at each end and at the one-third points.
26	Indication of the presence of supplementary steel (usually in the form of welded wire fabric)	0	No supplementary steel was present.
		1	Specimen contained supplementary steel.
27	Indicates spacing of mechanical shear transferring device, s, in inches	0	Mechanical shear transfer device (if present) was at a constant spacing and s is not a variable, e.g. embossment type of shear transfer.
		3	Indicates 3 in. spacing, e.g. spot-welded wires on 3 in. centers.
		4	Indicates 4 in. spacing.
		5	Indicates 5 in. spacing.
		6	Indicates 6 in. spacing.
		7	Indicates 7 in. spacing.
		8	Indicates 8 in. spacing.
28	Indicates whether steel deck was greased prior to concrete placement	0	Steel deck was not greased.
		1	Steel deck was greased.
29	Type of concrete	0	Indicates normal weight concrete.
		1	Indicates structural light-weight concrete.

A numerical code was used to indicate special variables regarding each individual test. If an assumption was made regarding any of the variables, this is given in the last column, along with any relevant notes.

2.3. Reports and Publications

To date, a total of seventeen published papers, two doctoral dissertations, one master's thesis, 27 progress reports, and five oral presentations have resulted from the ISU research. A complete listing to date of the published papers and theses is contained in the Appendix.

In addition, the research has resulted in a draft of "Tentative Criteria for the Design and Construction of Composite Steel Deck Slabs" and an associated commentary manual thereon. Final publication of these design criteria is anticipated by the Codes and Standards division of the American Society of Civil Engineers.

3. PUSHOUT TESTS

Initial phases of the research involved testing of horizontal and vertical types of pushout specimens. Examples of vertical pushout specimens are shown in Fig. 4. The tests were carried out by placing a hydraulic cylinder between the two concrete blocks, and merely pushing the two blocks apart. The purpose of these tests was to obtain data on the shear and bonding characteristics of the various types of steel decks.

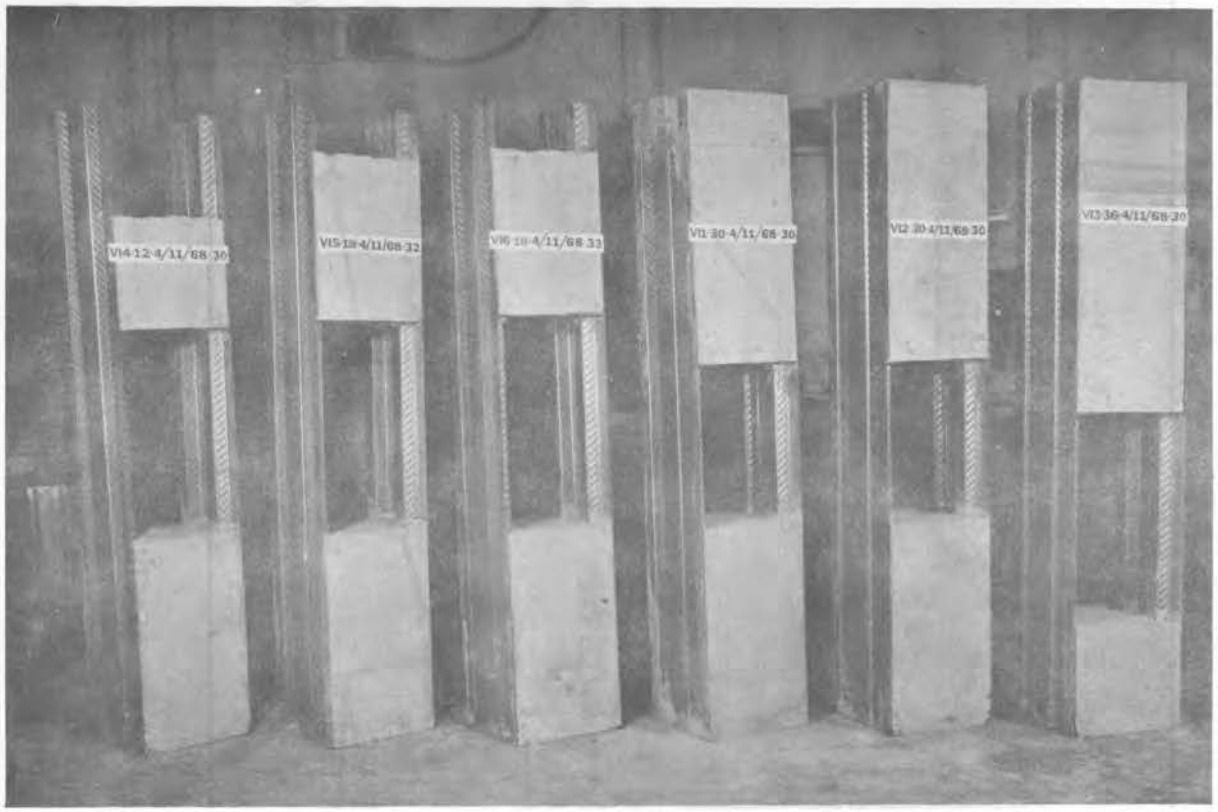

Fig. 4. Vertical pushout specimens.

Relationships between applied load and pushout displacement, steel strains, steel deck stress, and bond stress were obtained for the pushout tests. See [3]. Relationships for bond stress were also established as a function of embedment length, L'. An example of such a relationship for one deck type is shown in Fig. 5. The bond stress relationship, u', was based on an effective bonding area of the embossment plate elements, whereas the relationship, u, was based on the total bond area of

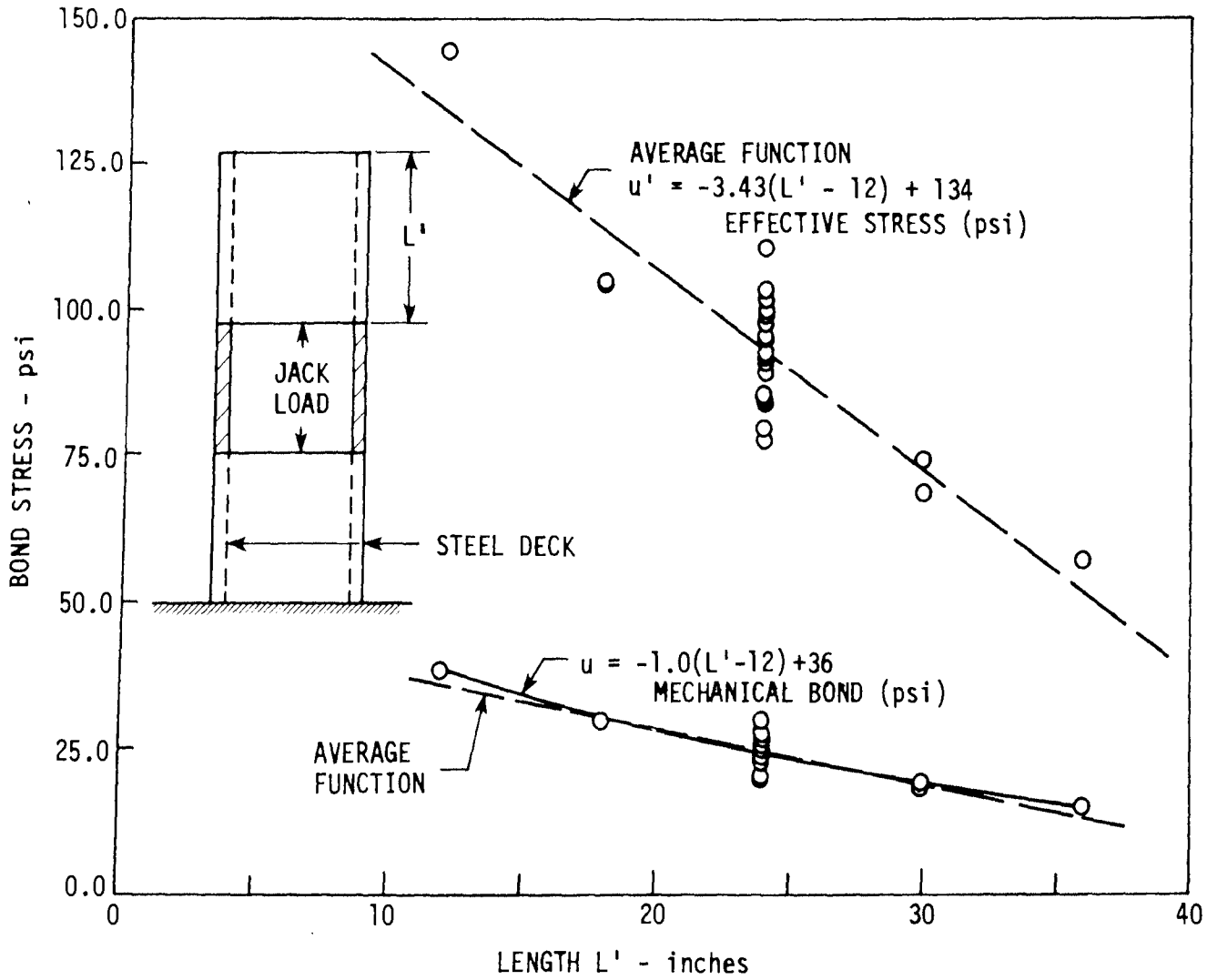

Fig. 5. Example of embedment length vs total mechanical bond and effective stress for pushout tests.

all deck surfaces. Relationships for other deck types and distortion measurements during failure are contained in [3]. Even though the pushout test specimens provided the aforementioned relationships for displacement, steel stress, bond stress, and embedment, a correlation of these relations and parameters to determine a direct computation of the shear and bond strength for flexural members did not result in a practical solution applicable to all deck types. Therefore, the strength of steel-deck-reinforced members was found directly from one-way slab element testing.

4. ONE-WAY SLAB ELEMENT TESTS

4.1. General

A total of 209 tests were conducted at Iowa State University on one-way slab elements for the purpose of determining the effects of ultimate strength of various parameters such as shear span, L', cross-sectional area of steel, A_s, effective depth, d, and others. These specimens were simply supported and contained various types of steel deck sections as reinforcement with the corrugations paralleling the span length (strong direction); see Fig. 6. All specimens, except those which sustained uniform loading, were subjected to either a single concentrated load at the center or two concentrated loads at a distance of L' from the supports. Most of the test members had a width equal to one normal steel deck panel as typically produced by the deck manufacturer. The nominal width varied from 1 to 3 ft, and out-to-out lengths and depths ranged from 6 to 16 ft and 3.5 to 5.5 in., respectively. Steel deck depths ranged from 1.25 in. to 3 in. and steel thickness ranged from 0.0251 to 0.0684 in. The above ranges in dimensions were chosen to include the spectrum of the more common span lengths, depths, and deck sections available to the designer.

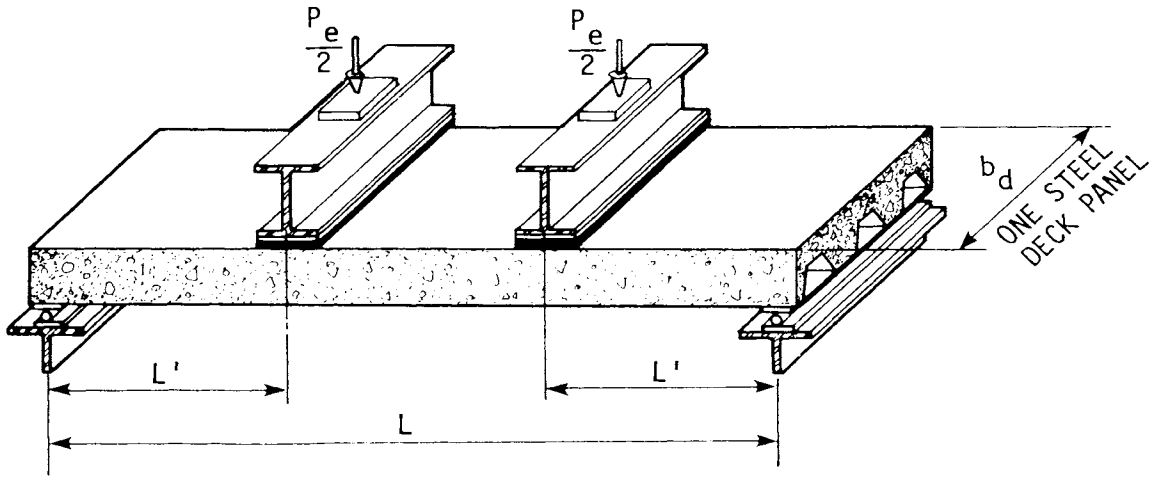

Fig. 6. Typical arrangement for testing one-way slab elements.

4.2. Description of Failure Modes

The results of the one-way steel-deck-reinforced slab element tests indicate that the primary modes of failure for slabs subjected to gravity

(vertical) loading may be classified as

1. shear-bond, and
2. flexure
   a. under-reinforced section
   b. over-reinforced section.

The ISU tests, along with numerous proprietary tests, indicate that the shear-bond failure mode is the one more likely to occur for most steel deck slab systems subjected to vertical loads. All but four of the ISU tests failed by way of the shear-bond mode of failure.

4.2.1. Shear-bond

The shear-bond mode of failure is characterized by the formation of a diagonal tension type of crack in the concrete at or near one of the load points, followed by a loss of bond between the steel deck and concrete resulting in visible slip at one end of the span (see Fig. 7). The term shear-bond was applied to this type of failure due to the simultaneous characteristics of both the shear and bond failures.

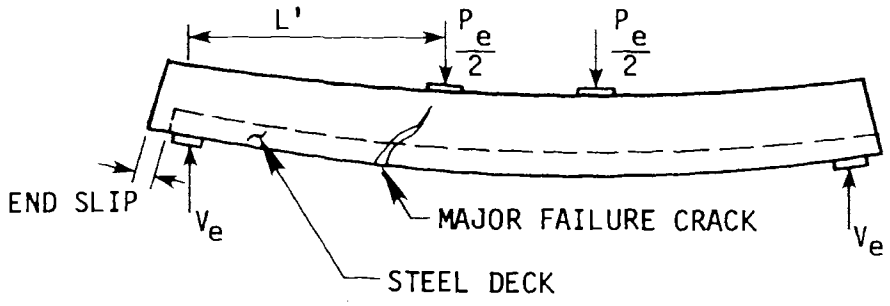

Fig. 7. Typical shear-bond failure.

Shear-bond failure results in a loss of composite action and horizontal slippage over the region of the shear span length, L', as shown in Fig. 7. The associated end-slip indicated in Fig. 7 results from the concrete moving horizontally, overriding or failing the shear transferring device, which consisted of embossments, spot-welded wires, or concrete protruding through holes in the steel deck. Normally, the visible end-slip occurred on only one end of the specimen as shown by Fig. 8.

Shear-bond failures were observed for shear spans ranging from 12 to 86 in. Figure 9 shows typical slab elements with varying shear spans, L', which failed by shear-bond. The arrows in Fig. 9 indicate the position of the applied line loads. Note that the failure crack

consistently occurred at or near the load point.

A significant behavioral observation was that shear-bond failures, characterized by end-slip, were sometimes accompanied by yielding of a portion of the steel deck cross section. Strain gages, placed on many of the specimens, indicated that shear-bond failure for the longer shear spans was preceded by yielding of the lower portion of the steel deck cross section, whereas no yielding of the steel occurred for the shorter shear spans. The longer shear-span test specimens generally approached a flexural behavior type of failure. In the case of deeper deck sections, however, the longer shear spans usually exhibited shear-bond failure characteristics, even though failure was preceded by yielding of the steel.

Shear-bond failures usually occurred abruptly and were followed by a significant drop in loading under the action of a hydraulic testing machine with constant head speed. The reduction of load-carrying capacity was due to a loss of bond as evidenced by end-slip. A few slab elements, however, exhibited a small amount of end-slip prior to ultimate load. Typical load versus end-slip displacement behavior is indicated at the left in Fig. 10. This plot demonstrates the most

Fig. 8. Photograph of end-slip after failure of a one-way slab element.

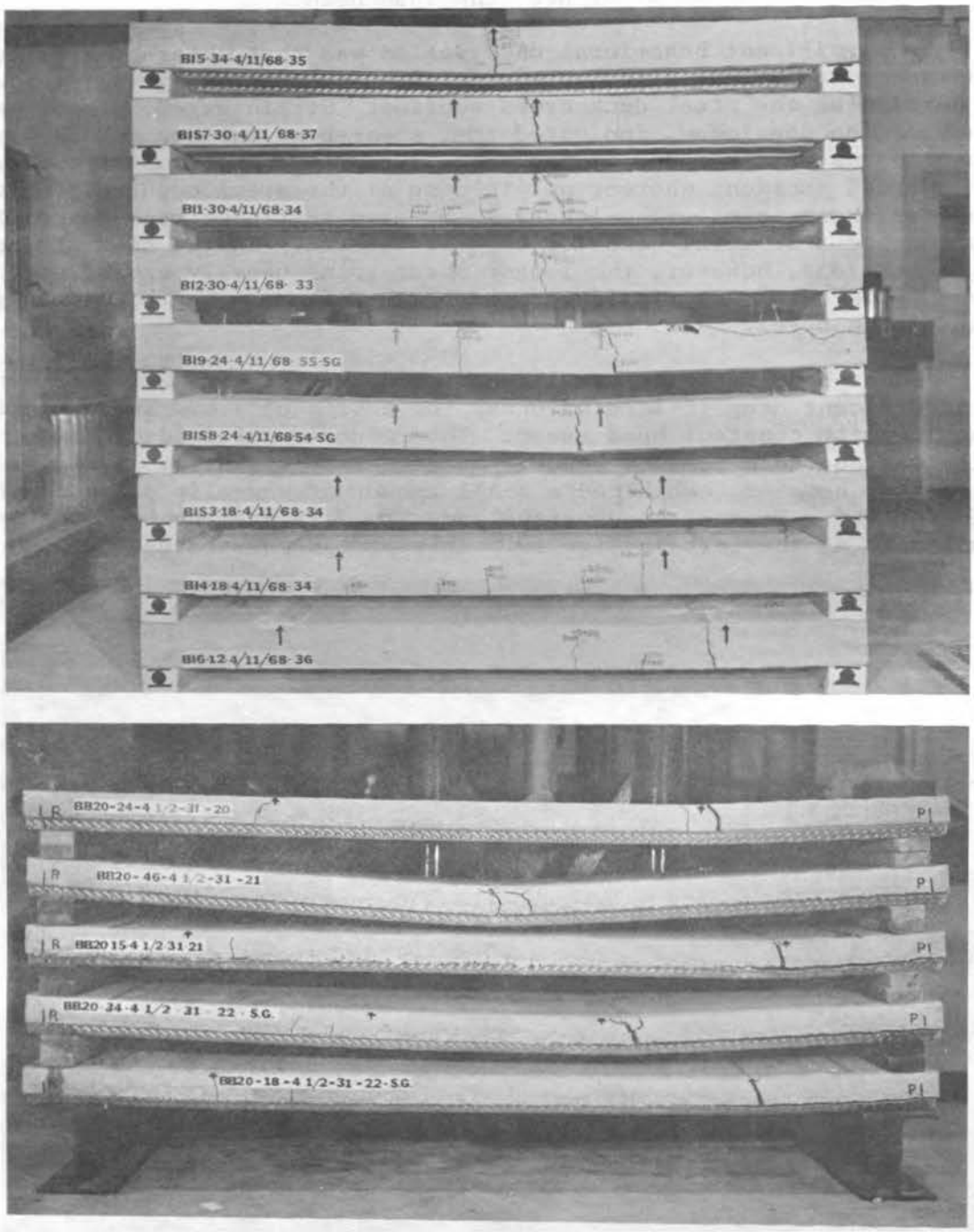

Fig. 9. Views showing one-way slab elements, with shear spans ranging from 46 in. to 12 in., which have failed in shear-bond.

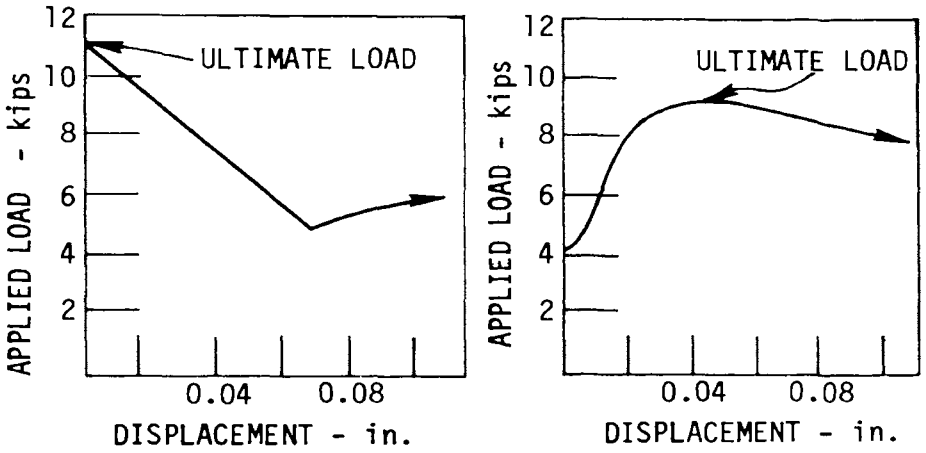

Fig. 10. Typical load-displacement relationships for end-slip.

common case where end-slip coincided with ultimate load. The plot on the right demonstrates an instance where end-slip occurred prior to ultimate load. Initial end-slip for this instance was detected at only 36% of the ultimate load. As would be expected, the early end-slip was followed by a noticeable reduction of stiffness.

In some cases, where early end-slip occurred, strain gages indicated yielding of the steel deck over part, or all, of the cross section. In one instance where the entire deck yielded, the specimen did not demonstrate the secondary compression failure associated with a normal under-reinforced flexural mode of failure. Instead, the mode of failure was more closely associated with shear-bond.

4.2.2. Flexure

The flexural failure modes for cold-formed steel-deck-reinforced slab systems depend on whether they are under- or over-reinforced. These two flexural failure categories are separated according to the balanced steel ratio, as developed from the conventional assumptions of compatibility of strains and equilibrium of internal forces. The tensile force is usually assumed to act at the centroid of the cross-sectional area of the deck for the cases where yielding of the entire steel deck cross section occurs. Flexural failures of steel-deck-reinforced systems are similar in behavior to those in ordinary reinforced concrete for under- and over-reinforced sections. Only four of the ISU tests failed completely by the flexural mode, three of which were classified as under-reinforced.

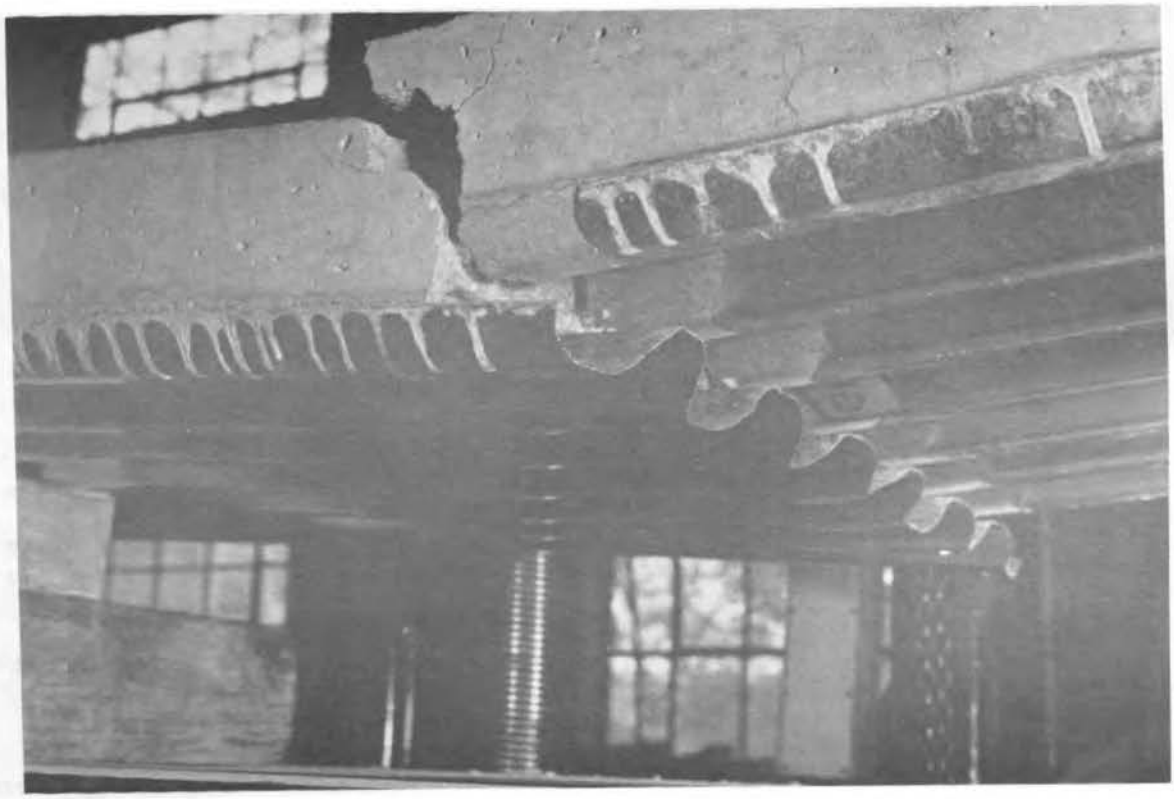

Fig. 11. View showing flexural failure of under-reinforced slab element.

Flexural failures of an under-reinforced slab element were primarily characterized by yielding and tearing of the entire deck cross section at the maximum positive moment section, as shown by the example in Fig. 11. The excess tensile strain in the steel was accompanied by one or more large cracks in the concrete. Conversely, failure of an over-reinforced slab element was characterized by a typical crushing failure of the top fibers of concrete at the maximum positive moment section. Only one over-reinforced failure was found from the ISU tests. The over-reinforced failure occurred suddenly and was not accompanied by an excess of steel strain.

5. DETERMINATION OF SHEAR-BOND STRENGTH

Many relationships have been developed for determining the shear-bond strength of a cold-formed steel-deck-reinforced slab element, such as that shown in Fig. 6. The basic parameters influencing shear-bond strength were found to be deck type; shear span, L', in inches; concrete compressive strength at time of test, f'_{ct}, in pounds per square inch (psi); cross-sectional area of steel deck, A_s, in square inches per foot of width, or reinforcement ratio, $\rho = A_s/bd$; specimen width, b, in inches; the distance, d, in inches, from the extreme compressive fiber to the centroid of the steel deck cross-section at the point of failure; and, s, the spacing of shear transferring devices, in inches. For those instances where the shear transferring device is a fixed pattern for all deck sections of a particular profile, such as for embossments, the spacing, s, is simply taken as unity. An s-value of unity is also used where the composite action is provided by a combination of the deck profile and the surface bond. Deck profiles containing shear interlocking devices, such as holes and transverse wires, have a spacing, s, in inches, equal to the center-to-center distance between such devices. For example, on one deck sheet all transverse wires might be spaced at 3 in. centers, whereas on another deck of the same profile, the spacing might be at 6 in. centers. Thus, the s-values would be 3 and 6 in., respectively. The term, s, has not been defined for a deck where the spacing of the shear device varies along a single deck panel. Current practice does not include decks of this type.

The strength relationships are based on the fact that values of maximum experimental shear at failure, V_e, for a given deck type can be combined with the basic parameters to provide a linear equation. Such a linear relationship is shown in Fig. 12, and is given by

$$\frac{V_e s}{bd} = \frac{m_1 \rho d}{L'} + k_1 \sqrt{f'_{ct}} \qquad (1)$$

where

m_1 = slope of shear-bond regression line
k_1 = ordinate intercept of shear-bond regression line

The reliability of the regression line in Fig. 12, and correspondingly the values of m_1, and k_1, depends on the number of available data points.

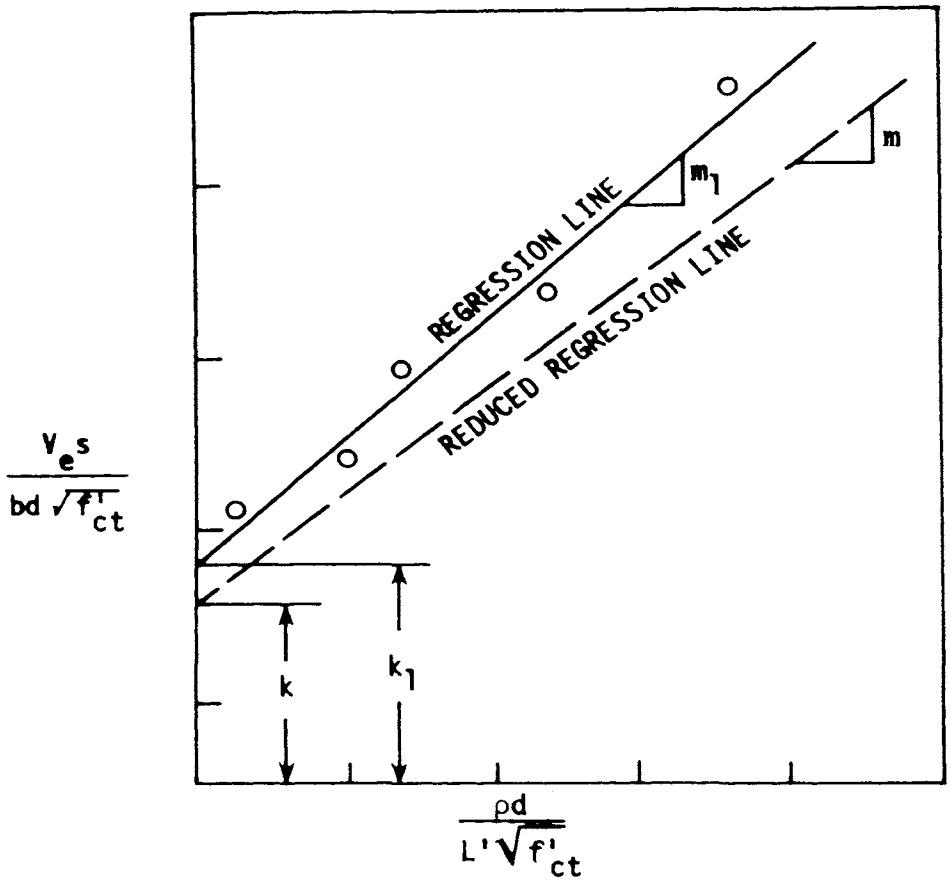

Fig. 12. Typical shear-bond plot showing the reduced evaluation of m and k.

5.1. Strength Prediction Equations

Once the values of m_1 and k_1 have been determined for a particular deck type, the ultimate shear-bond capacity, V_u, in pounds per foot of width can be computed. This can be accomplished by revising Equation (1) as follows:

$$\frac{V_u s}{bd} = \frac{m\rho d}{L'} + k\sqrt{f'_c} \qquad (2)$$

where

m = reduced slope of shear-bond regression line
k = reduced ordinate intercept of shear-bond regression line
f'_c = specified strength of concrete

The reduced slope and intercept ensures that the experimental values will generally fall above the design values. The reduction accounts for any minor variations in the laboratory test specimens, e.g. deck profile, steel thickness, and other dimensions. Thus, Equation (2) is represented by the reduced regression line in Fig. 12, and m and k are 15% less than the corresponding values m_1 and k_1. Conceivably, a 10% reduction would be appropriate if a sufficiently large number of tests were conducted to establish the regression line.

For convenience, Equation (2) can be rearranged as follows:

$$V_u = \frac{bd}{s}\left[\frac{m\rho d}{L'} + k\sqrt{f'_c}\right] \tag{3}$$

to give direct values of the ultimate shear, V_u. An additional term, $\gamma W_1 L/2$, can be added, representing the amount of dead load applied to the composite member, in pounds per square foot (psf), and where L is the span length in feet. The coefficient, γ, represents that portion of the dead load which is applied upon removal of shoring (if present). For example, if a composite deck system is cast having a single shore as a line support at the center of a simple span, then the amount of dead load acting on the composite system upon removal of shoring is the shore reaction of (5/8) × $W_1 L$. The resulting end shear is 5/8 ($W_1 L/2$), and thus γ is simply 5/8. Likewise, if no shoring is used, γ is zero. If the slab system is continuously supported throughout its entire length during the casting process, γ is equal to 1.0.

For uniformly applied loads, the L' in Equation (3) can be taken as one-fourth of the span length, L (as verified by uniformly loaded tests which are discussed later in this bulletin). Using a unit width of the slab element of 12 in., substituting for L', and adding the dead load term, Equation (3) can be written as

$$V_u = \frac{d}{s}\left[\frac{4m\rho d}{L} + 12\ k\sqrt{f'_c}\right] + \frac{\gamma W_1 L}{2} \tag{4}$$

Design recommendations have been formulated which include Equation (4) as well as several other design considerations, see [4]. These design recommendations were developed in conjunction with the AISI's Task Committee on Composite Construction and are entitled "Tentative Criteria for the Design and Construction of Composite Steel Deck Slabs." A commentary manual containing explanations for the Design Criteria was also prepared (see the Appendix, listing No. 8).

5.2. Example Shear-Bond Formulations

Many equations for shear-bond were utilized in a regression formulation in order to establish which one was most suitable. Three example relationships considered to be most typical are shown in Table 3. Details of shear-bond analysis results for these equations are presented below and in [5].

Table 3. Possible equations for shear-bond failure.

Equation number	Form of regression equation	Experimental X value	Experimental Y value
A	$\frac{V_u s}{bd} = \frac{md}{L'}\sqrt{f'_c} + k\rho$	$\frac{\sqrt{f'_{ct}}(d)}{\rho L'}$	$\frac{V_e s}{bd\rho}$
B	$\frac{V_u s}{bd} = \frac{m\rho d}{L'} + k\sqrt{f'_c}$	$\frac{\rho d}{\sqrt{f'_{ct}}(L')}$	$\frac{V_e s}{bd\sqrt{f'_{ct}}}$
C	$\frac{V_u s}{bd} = m\left(\frac{f'_c \rho d}{L'}\right)^{1/3} + k$	$\left(\frac{f'_{ct}\rho d}{L'}\right)^{1/3}$	$\frac{V_e s}{bd}$

Equations (A) and (B) in Table 3 are based on the hypothesis that failure is initiated by diagonal tension cracking. A derivation of Equation (A) is given by R. M. Schuster [6]. Equation (B) is of the form of the shear equation in the American Concrete Institute (ACI) Building Code [7]. Equation (C) was developed by Zsutty [8] utilizing dimensional analysis, where the exponent of one-third was determined by statistical analysis of shear failures in reinforced concrete beams.

A comparison was made of the relative reliability of Equations (A), (B), and (C) as well as several other equations by utilizing all available data. Each of the test specimens had a total of 29 associated variables, which included steel deck type and cross section properties, shear span (L'), ultimate applied load (P_e), dead load, type of failure, span length, type of loading, specimen width (b), depth (d), concrete compressive strength (f'_{ct}), spacing of mechanical shear transferring devices (s) and shoring condition. A computer program was written to perform a linear regression analysis, i.e., the determination of m_1 and k_1 (slope and intercept, respectively) from the experimental data.

The computer program assembled the specimens into groups with as many as seven common variables in one particular grouping. For example, all slabs with a common deck type and surface condition were grouped together. The computer program also calculated average percent errors (absolute value), correlation coefficients, confidence intervals for the data points and regression lines, and statistical test values. In addition, standard deviations of a sample and of a regression slope were considered. By comparing these quantities, the validity of each equation was evaluated.

Each of the coefficients in the equations, relating to shear-bond type failures, was found from a regression analysis of the available data. Since none of the equations included the effects of deck type, surface condition, or shoring condition, these variables were eliminated from consideration by appropriate grouping of specimens. Only results of shear-bond failures were used (i.e., flexural failures were eliminated).

The specimens were further grouped such that each linear regression aggregation had the common variables listed in Table 4. The groups in Table 4 are divided into three categories denoted by Case 1, Case 2, and Case 3. The three cases differ only with respect to deck thickness and shoring condition. Each of the Case 1 groups had a combination of deck thicknesses, but only one type of shoring condition. The groups of Case 2 had only a single deck thickness and a single shoring condition per group, whereas each group of Case 3 had a combination of deck thicknesses and a combination of shoring conditions.

Shoring conditions of the steel deck during the construction stages of the specimens provided a means of separating groups of specimens as indicated in Table 4. Three shoring support situations were employed, namely:

1. completely supported throughout the entire specimen length,
2. no shore supports, and
3. one concentrated line shore support extending across the specimen width at approximately the center of the span.

Each shoring condition subjected the composite slab section to a different dead weight loading situation when shoring was removed. A correction for the shoring condition will be discussed later in this bulletin.

The experimental live load shear, V_e, equals $P_e/2$, where P_e is simply the experimental ultimate applied load. Admittedly, dead load must be incorporated into the design equation, and this is studied in the following section. However, a satisfactory comparison of the relative merit of the various design equations was obtained by neglecting dead load.

Table 4. Common variables for linear regression groups.

Variable	Grouping based on deck thickness and shoring condition[a]		
	Case 1	Case 2	Case 3
Gage thickness of steel deck	All thicknesses	One thickness	All thicknesses
Shoring condition	One type of shoring condition	One type of shoring condition	All types of shoring condition

[a]For each case, linear regression groups had common deck type, failure type (shear-bond), load type, and surface condition.

The average percent error is

$$\text{percent error} = \frac{1}{n} \sum \frac{|d_{y \cdot x}|}{Y} (100)$$

where n is the number of specimens in a group, $d_{y \cdot x}$ is the deviation of a particular data point from the regression line, and Y is the ordinate of the data point. In the previous equation the ordinate of the data point was used as the basis for determining the average percent error, since that value is considered more accurate than the ordinate of the regression line, which is the average representation of several design parameters. The correlation coefficient, r, is

$$r^2 = 1 - \frac{\Sigma \left(d_{y \cdot x}\right)^2}{\Sigma (Y - \bar{Y})^2}$$

where $\bar{Y}$ is the mean of Y.

After the specimens were subdivided with the common sort of variables summarized in Table 4, a linear regression analysis was performed on each group to determine the constants m and k. The average percent error and correlation coefficient was obtained for each case. Table 5

summarizes the results for each of the three example cases for the ISU tests.

The values of Table 5 must be interpreted with care since the average percent error includes all specimens which were involved in the various linear regression analyses. Thus, when all gages were grouped together (Case 1), some groups had only one gage thickness. The average percent error of these groups is also incorporated into the Case 1 values. Similarly, other groups in Case 1 had an unequal number of the various gage thicknesses, e.g., 15 specimens of 16 gage, 47 specimens of 18 gage, and 45 specimens of 22 gage. This tends to weight the regression analysis toward the gage thickness with the most specimens. No simple method was developed for eliminating this effect. One can expect, however, that the effect is similar for all equations and therefore Table 5 can yield satisfactory comparisons.

Table 5. Results of linear regression analyses showing average percent errors and correlation coefficients.

	Average percent error (and correlation coefficient)		
	Case 1	Case 2	Case 3
Equation number	All thicknesses; one shoring condition	One thickness; one shoring condition	All thicknesses; all shoring conditions
A[a]	11.3 (0.93)	7.8 (0.95)	12.5 (0.94)
B	10.1 (0.91)	7.4 (0.94)	12.5 (0.90)
C	10.9 (0.90)	9.3 (0.92)	11.8 (0.90)

[a] See Table 3 for equations.

A total of 40 specimens were "retested". These retested specimens were obtained by utilizing the unfailed portion of a previously tested longer specimen. Due to the large scatter of the retest results and the unknown question of previous specimen damage from prior testing, these retest specimens were omitted from the results in Table 5 and from subsequent results shown in this bulletin. Furthermore, the above retest rejection leads to the recommendation that retest specimens not be utilized as a means of gathering additional test data.

A comparison of Cases 1 and 2 in Table 5 indicates how well each equation accounts for the steel percentage (or area, or thickness). The loss of accuracy if a common equation is used for all gage thicknesses is evident. Thus, the average total percent error increases by 2.7% if Equation (B) is used with a constant m and k for all gage thicknesses (Case 1), as compared to a different m and k for each gage (Case 2). This means that the designer can use the same design equation for all gages if he is willing to accept a possible increase in the total error of 2.7%. The designer is cautioned, however, that certain deck types are quite noticeably affected by a change in gage thickness. Examination of Table 5 shows that if one equation (one set of m and k) is used for all gages the accuracy of Equation (B) for Case 1 is also superior to the other equations.

Case 3 in Table 5 indicates the effect of combining all shoring conditions. As can be seen, a higher percent error occurs when all shoring conditions are combined. A correction to account for the shoring condition is discussed in the following section.

Table 5 summarizes the accuracy of the prediction for each of the three cases for the ISU tests. Similar results were obtained from the proprietary tests conducted by various steel deck manufacturers. Case 3 yielded the highest average percent error; however, the percents of Case 1 were almost as high. A significant observation is that the best values were achieved with the groups of Case 2, in which there was only a single deck thickness and one type of shoring condition.

Based on the results of Table 5, Equation (B) is recommended for design. The percent errors of Equation (B) are consistently lower than those for Equations (A) and (C). The correlation coefficients range between 0.90 and 0.95 and give slightly better results for Equation (A). The percent errors were felt to give a more significant basis for the equation selection than the correlation coefficients. Equation (B) has the additional advantage of familiarity to the design profession.

The typical quality of fit of Equation (B) is illustrated in Figs. 13-16. In these example figures, the experimental data points are plotted for a particular deck type representing the variables listed in Table 2 for Case 1 (Cases 1 and 2 for Fig. 13). A linear regression line together with lines representing plus or minus 15% deviation intervals from each regression line are shown in each figure.

The plots shown in Figs. 13-16 represent six different manufactured steel decks and are typical of the results obtained. These figures, together with the results shown in Table 5, provide a quantitative mea-

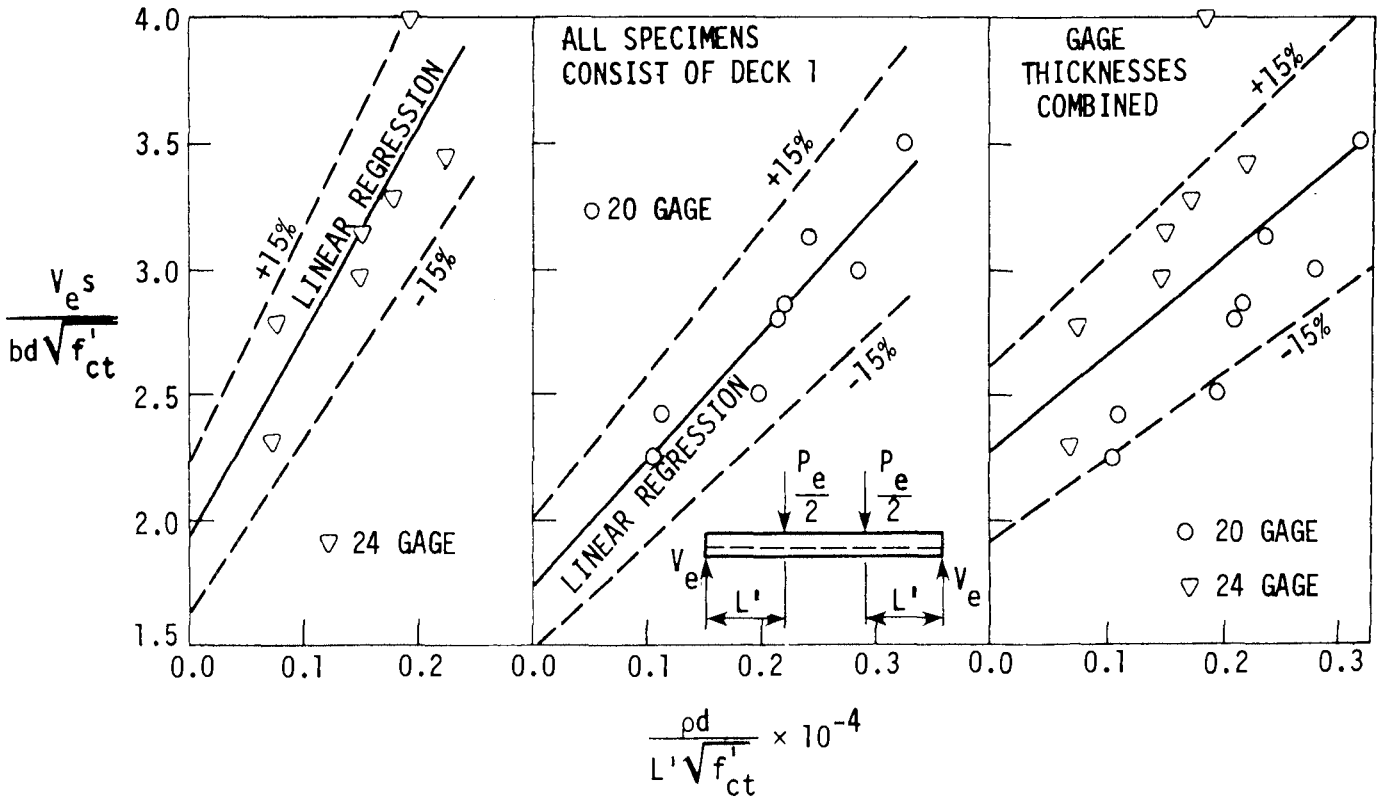

Fig. 13. Example plots illustrating the effect of gage thickness for Equation B utilizing Deck 1.

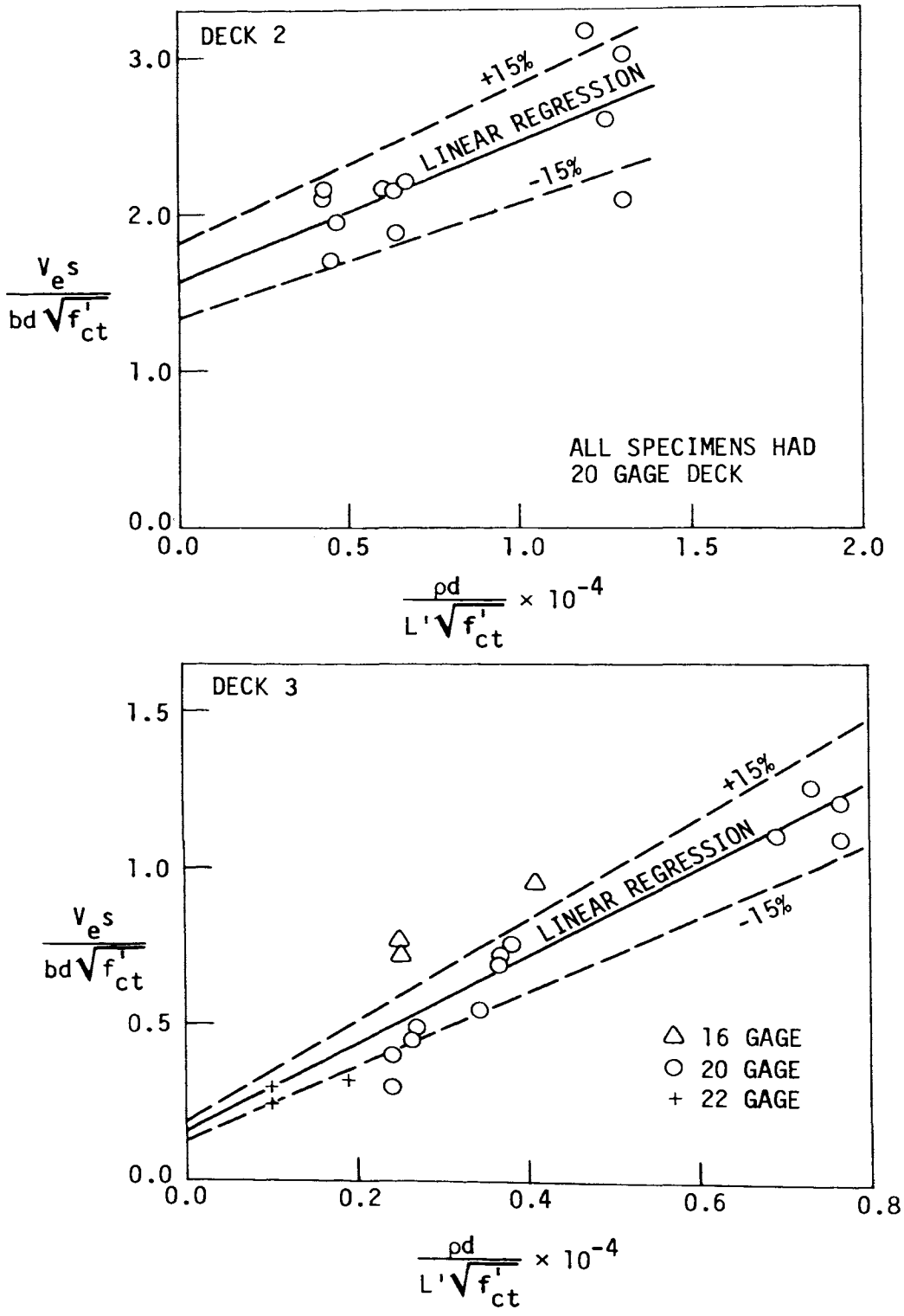

Fig. 14. Example regression plots for Equation B utilizing Decks 2 and 3.

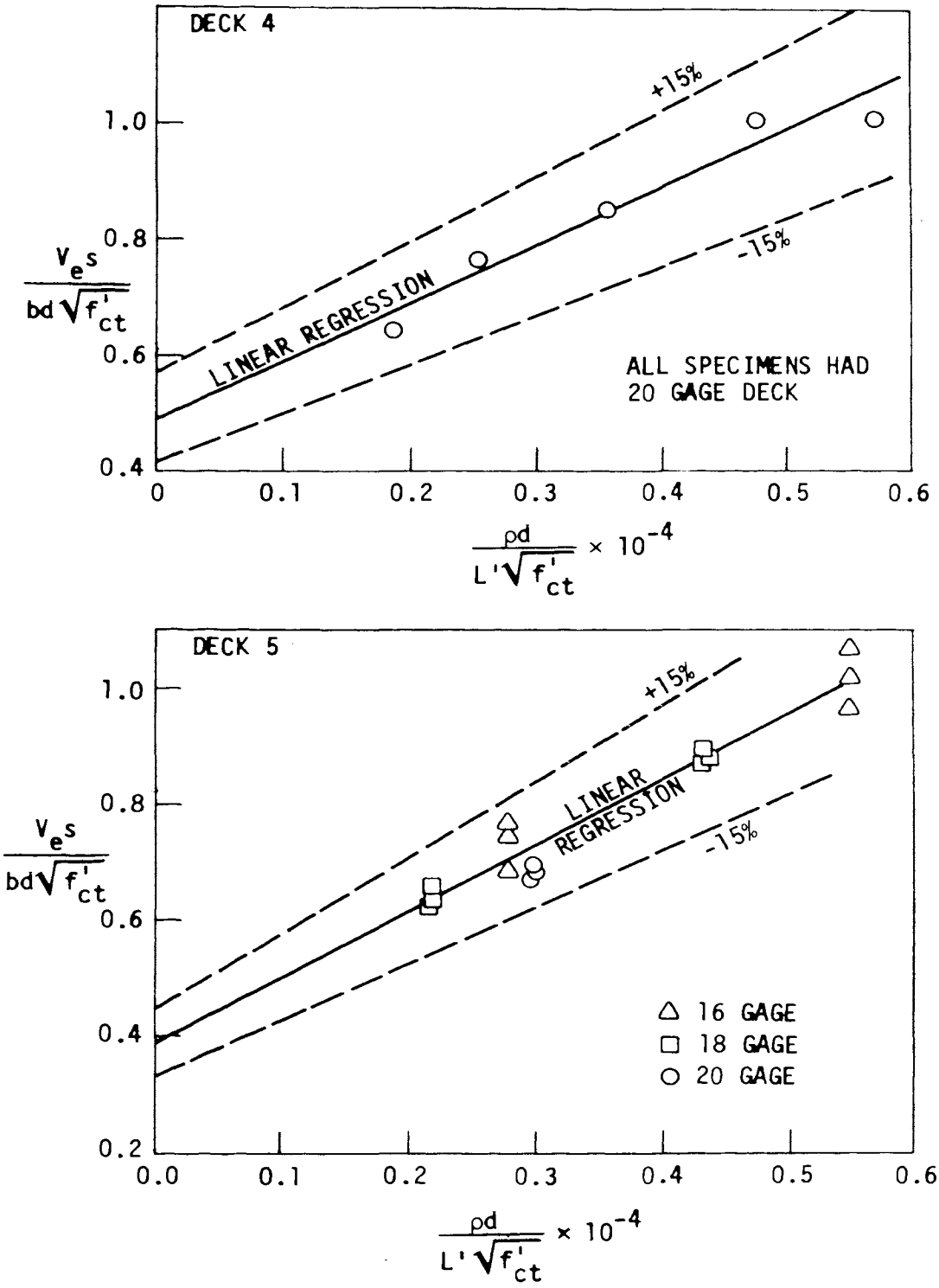

Fig. 15. Example regression plots for Equation B utilizing Decks 4 and 5.

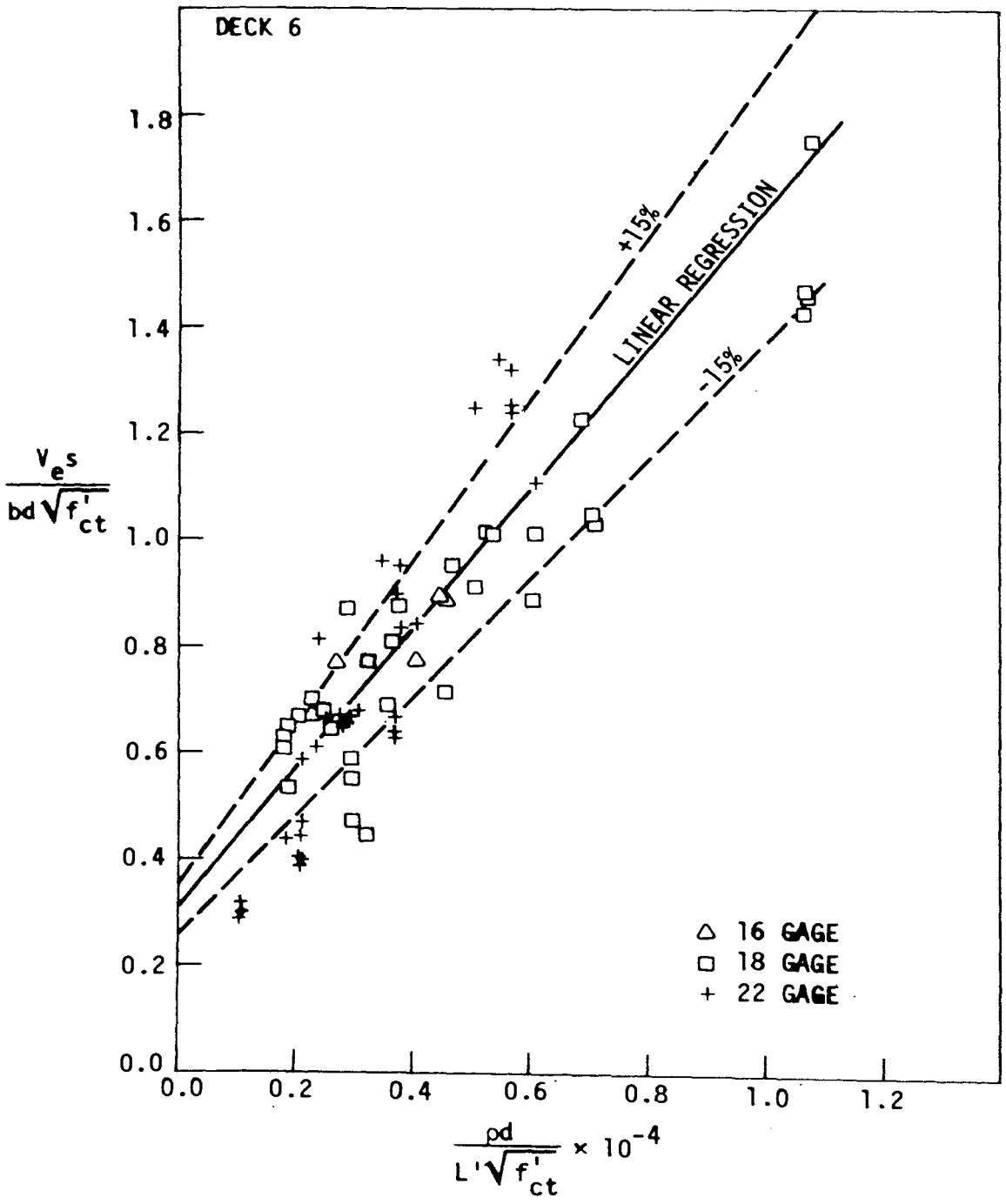

Fig. 16. Example regression plot for Equation B utilizing Deck 6.

sure of the accuracy of Equation (B) in predicting the ultimate shear force.

Gage thickness changes affect certain steel-deck-reinforced slabs more significantly than others. This result can be seen by looking at the various gages shown in Figs. 13-16 as shown by Decks 1, 3, 5, and 6. The diagrams in Fig. 13 indicate that there is a definite change in the regression constants m and k as gage thickness changes. A composite diagram shown in Fig. 13(c) illustrates a much greater scatter for a combination of gage thicknesses; however, the plus or minus 15% regression deviations come close to including both the 20 and 24 gage thicknesses. Note particularly that the three 16 gage points for Deck 3 in Fig. 14 are all higher than the other gages.

5.3. Comparison of Theoretical and Experimental Results

Equation (4) can be re-written for design in the following form to give the calculated ultimate shear, V_u, in pounds per foot of width:

$$V_u = \phi\left[\frac{12d}{s}\left(\frac{m\rho d}{L'} + k\sqrt{f'_c}\right) + \frac{\gamma W_1 L}{2}\right] \tag{5}$$

where

ϕ = shear-bond capacity reduction factor = 0.80
γ = portion of dead load added upon removal of shore,
W_1 = slab dead load, psf

Utilizing the load factors in the ACI Building Code [7], the allowable superimposed live load (LL) in psf is:

$$LL = \frac{1}{1.7}\left[\frac{2V_u}{L} - 1.4\left(\gamma W_1 + W_3\right)\right] \tag{6}$$

where

L = span length, feet
W_3 = dead load applied to slab exclusive of W_1, psf

Based upon design Equations (5) and (6), several illustrative examples will be presented. As a means of indicating the validity of the predicted results, the experimental load-deflection relationships for slab elements constructed with 16, 18, and 20 gage deck will be utilized. See Figs. 17 and 18. The experimental deflections were measured at midspan and represent the maximum vertical displacement at each applied loading increment. Indicated on each curve is a horizontal line corresponding to the allowable live load (ALLOW LL) as obtained from Equation (6). The constants m and k in Equation (5) were obtained from linear regressions shown in Fig. 19, where data from tests on slab elements is plotted separately according to gage thickness. All specimens in Figs. 17-19 were reinforced with a 3 in. deep steel deck having embossments as the means of shear transfer between the deck and concrete. The nominal width and out-to-out depth was 36 in. by 5.5 in. and the lengths varied from 6 to 16 ft. The concrete had an average compressive strength of approximately 4,000 psi. Other pertinent data used in Equations (5) and (6) is indicated in Figs. 17-19.

Figures 17 and 18 show that each of the computed allowable live load values seem to be reasonable, in that they define a fairly straight-line portion of the load-deflection curves. Thus, the computed live load seems to provide a consistent and reasonable margin of safety for all the test members.

Figure 17 exhibits load-deflection behavior for specimens reinforced with the same gage thickness of steel deck, but with varying shear spans and span lengths. Note that the behavior changes considerably from a short to a long shear span. The slab elements exhibit considerable stiffness with little ductility when the shear span is short. However, the long shear span (and span length) induces much more ductility and considerable nonlinearity. A significant observation is that the computed allowable load (ALLOW LL) provides consistent results for each type of load-deflection relationship, i.e., decreasing load with increasing shear span and span length.

Figure 18 presents load-deflection relationships for specimens reinforced with three different gage thicknesses of steel deck, but having the same shear span and span length. The nonlinearity is observed to increase slightly with decreasing thickness of the steel. Again, note that the computed live load apparently provides a reasonable working range.

Figures 17 and 18 include a vertical line indicating the allowable deflection limitation of 1/360 of the span length. As can be seen, the load-deflection behavior is a fairly straight-line relation to the left of this allowable deflection limitation. In addition, the 1/360 of the span length limitation is significant in comparison with the computed allowable live load. In most cases the allowable LL value was close to or within the 1/360 limitation, indicating somewhat of a "balanced" design with respect to deflections.

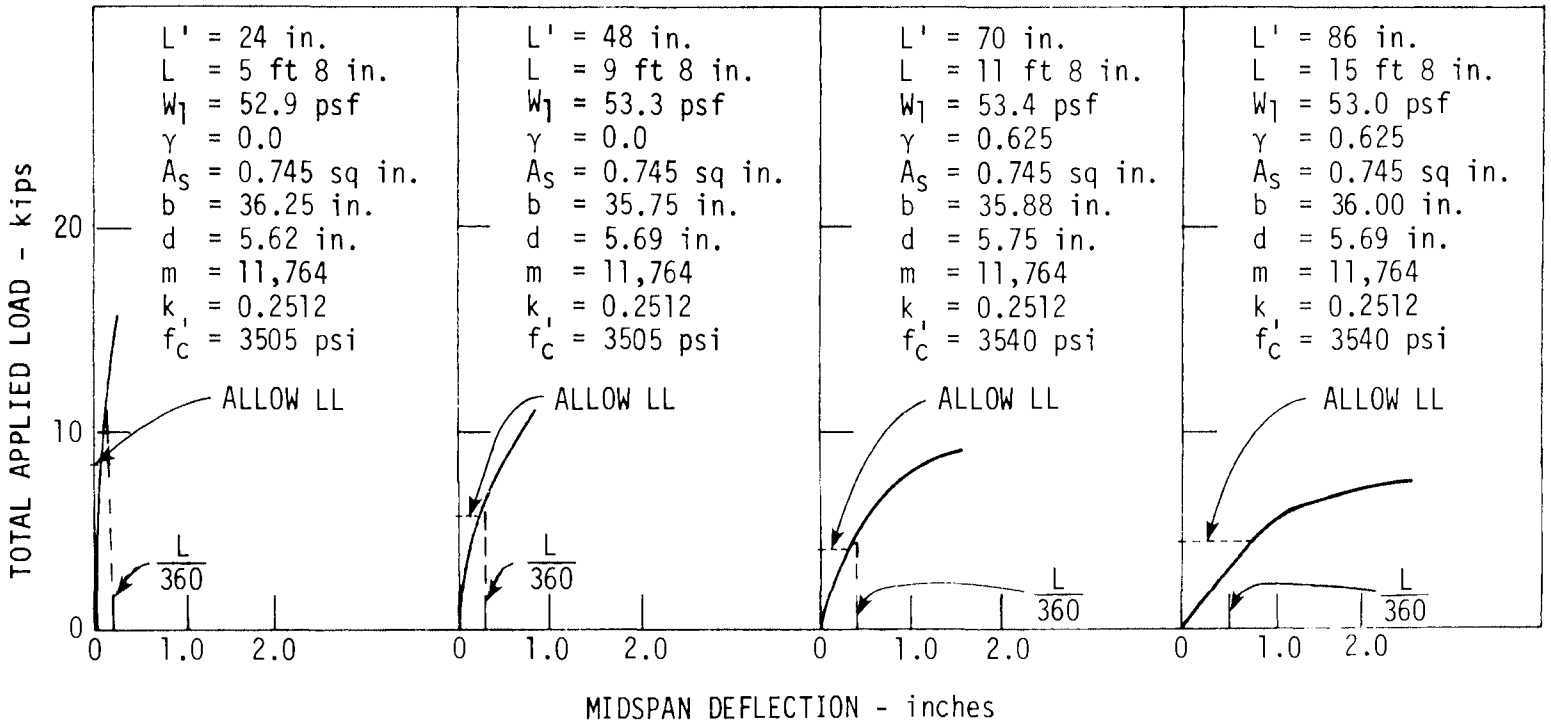

Fig. 17. Example load-deflection relationships of various shear spans and span lengths showing the allowable live load for specimens reinforced with 18 gage steel deck.

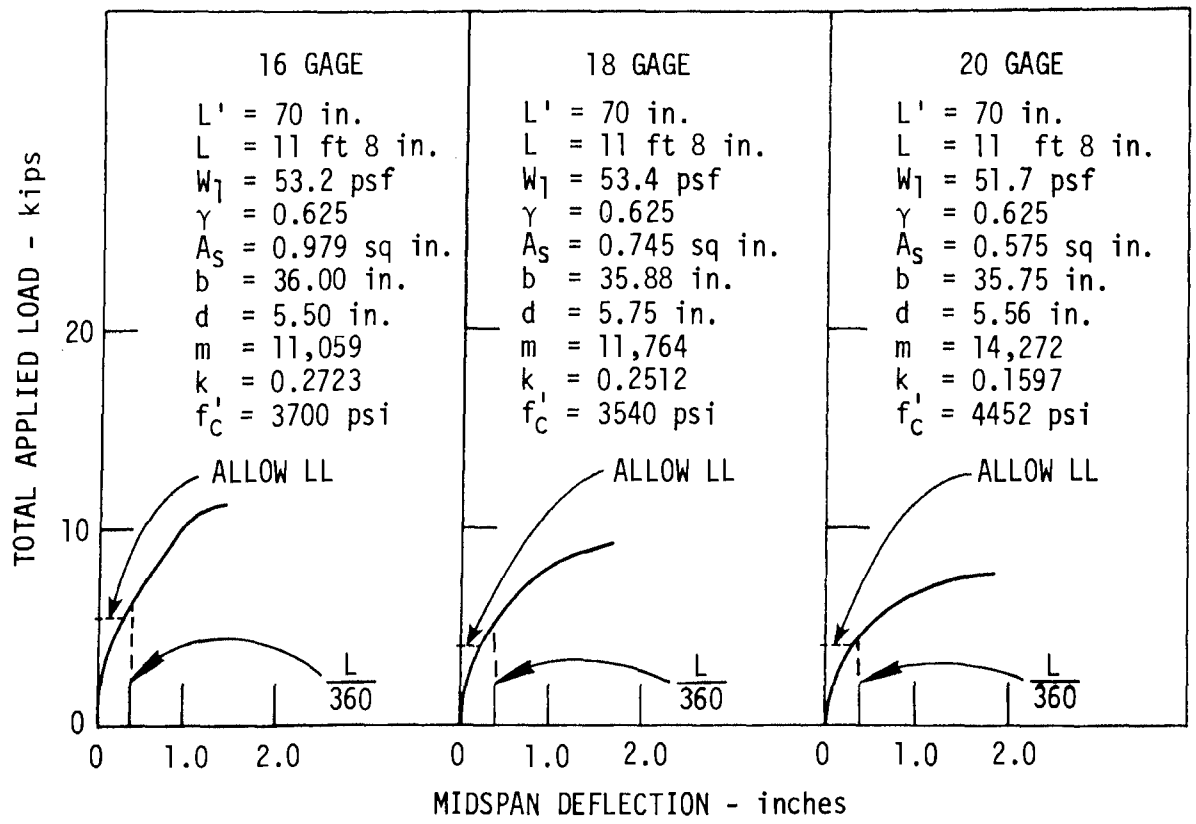

Fig. 18. Example load-deflection relationships showing the effects of specimens reinforced with different gage thicknesses of steel deck.

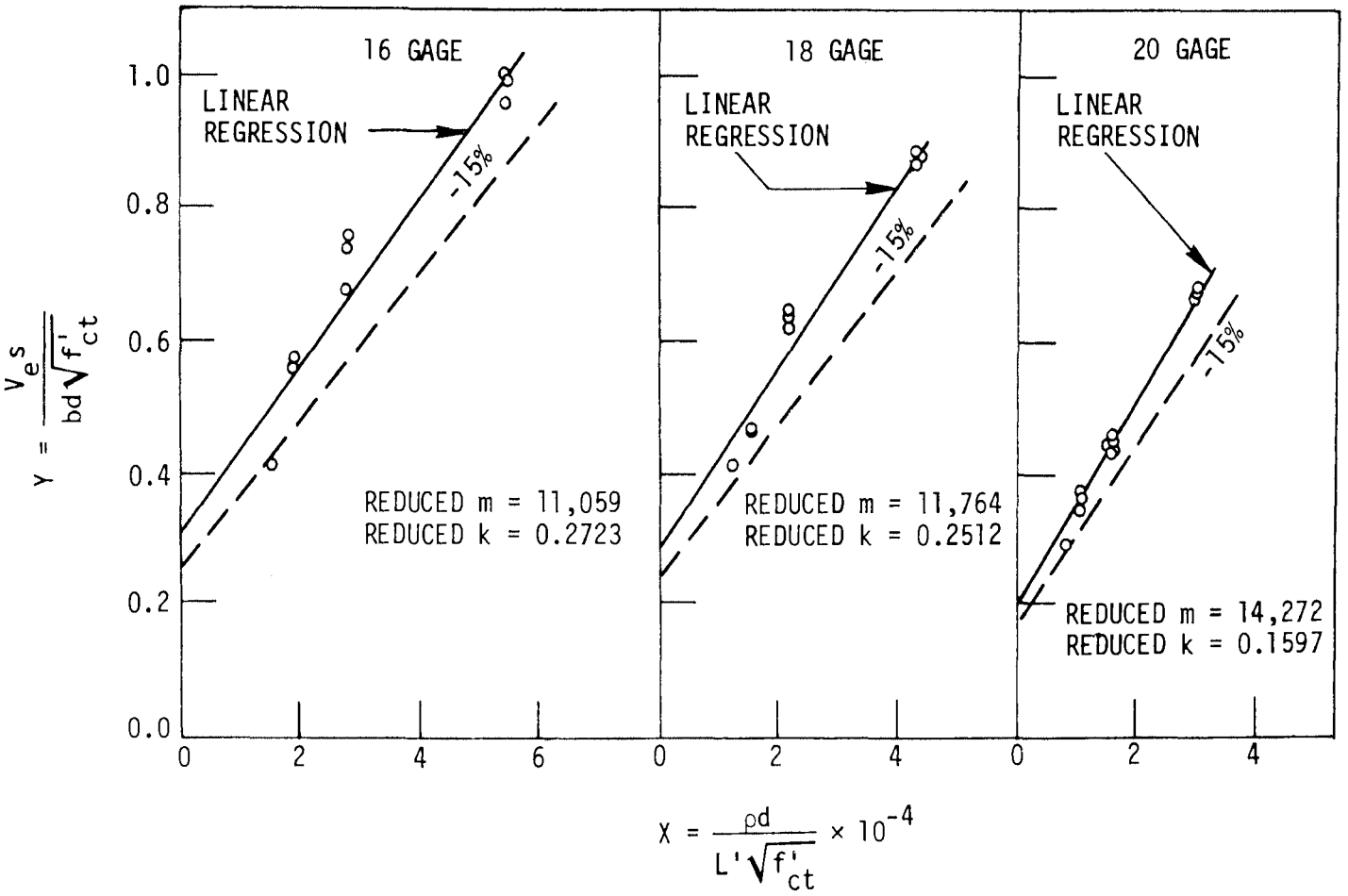

Fig. 19. Linear regression relationships for obtaining design live loads indicated in Figs. 17 and 18.

6. DETERMINATION OF FLEXURAL STRENGTH

6.1. Conventional Methods

The method prescribed in the ACI Building Code [7] for determining the flexural strength of reinforced concrete members is assumed to be applicable for most composite steel deck slabs. In the typical case where the steel deck serves as tension reinforcement and the corrugations are oriented in the direction of the span, the flexural computation is classified as under- or over-reinforced depending upon the reinforcement ratio, $\rho = A_s/bd$. The ratio that denotes a balanced condition for steel deck slabs is

$$\rho_b = \frac{0.85\ \beta_1\ f'_c}{F_y}\left[\frac{87{,}000\ (D - d_d)}{(87{,}000 + F_y)d}\right] \tag{7}$$

where

β_1 = 0.85 for concrete with $f'_c \leq 4000$ psi, and is reduced at a rate of 0.05 for each 1000 psi of strength exceeding 4,000 psi, but β_1 shall not be less than 0.65
f'_c = compressive strength of concrete, psi
F_y = yield point of steel, psi
D = nominal out-to-out depth of slab, in.
d = effective slab depth, in.
d_d = overall depth of steel deck profile, in.

Slabs with $\rho \leq \rho_b$ are considered under-reinforced, and the assumed predicted ultimate moment capacity, M_u, in ft-lbs/ft of width is found from

$$M_u = \frac{\phi A_s\ F_y\ (d - a/2)}{12} \tag{8}$$

where

ϕ = Flexural under-reinforced capacity reduction factor, taken as $\phi = 0.90$
A_s = cross sectional area of steel deck where used as tension reinforcement, $in.^2$/ft of width
$a = \dfrac{A_s\ F_y}{0.85\ f'_c\ b}$
b = width of slab element, in. (usually 12 in.)

The following conditions are assumed to be applicable with regard to Equations (7) and (8):

1. The entire steel deck profile has reached yield stress, without rupture;

2. The location of the resultant tensile force in the steel deck coincides with the centroid of its cross-sectional area;

3. The concrete reaches a maximum compressive strain of 0.003 at its outermost fibers;

4. No additional layers of tension steel reinforcement exist.

Slabs with $\rho > \rho_b$ are considered as over-reinforced. Calculation of the over-reinforced flexural mode is more complex than conventional reinforced concrete, in that the resultant tensile force in the steel deck does not coincide with the centroid of its cross-sectional area. This stems from the fact that the stress at the top fiber of the deck may be significantly less than the stress at lower fibers.

Computation of the flexural capacity for the over-reinforced cases and for cases when Equation (8) is not valid may be found by use of a "General Strain Analysis" technique based upon strain compatibility and equilibrium, as discussed in the next section. In this instance the factor ϕ is recommended as 0.70.

6.2. General Strain Analysis

In some instances, the usual assumptions applied to Equations (7) and (8) are not all valid. The more common occurrences could include the following.

1. The entire steel deck cross section has not reached yield stress at the instant of the flexural moment capacity. This condition may occur in those slab sections where a larger deck depth constitutes a very high percent of the total slab depth. In this situation the following events might lead to failure:

   a. rupture (tearing) of the bottom steel fibers,
   b. maximum concrete compressive force exceeded (crushing of concrete), or
   c. buckling of top fiber of steel deck cross section (if in compression zone).

2. The centroid of the steel deck cross-sectional area may not be sufficiently close to the resultant force carried by the steel. This condition may occur when

   a. the entire steel deck section does not yield,
   b. supplementary steel exists in addition to the steel deck, or
   c. the effective compression plate element widths are less than the full width (as per cold-formed design specifications [9]).

3. The concrete does not reach the assumed maximum strain of 0.003 in./in. This may take place, for example, if the steel deck reaches its rupture stress prior to the concrete reaching its capacity.

4. The concrete reaches its compressive strength prior to the entire cross section of the steel deck reaching its yield. This condition may occur for slabs where the deck depth is a very high percent of the overall slab depth.

5. The outermost steel deck tension fibers may rupture prior to the concrete reaching a strain of 0.003. This condition may occur when the steel deck consists of a very high strength, low ductile steel.

6. The steel deck slips horizontally with respect to the concrete, but the ultimate failure mode is still that of flexure. This case means that the usual assumption of strain compatibility may not be valid.

7. The designer wishes to account for the locked-in strains due to casting and shore removal.

A general strain analysis technique may be used to calculate the flexural capacity when Equation (8) can not be used and also provides a means of accounting for the "locked-in" strains due to casting and shoring conditions. The technique is based upon strain compatibility across the entire cross section and upon equilibrium of internal forces.

Figure 20 shows example strain diagrams that may be superimposed to obtain the flexural capacity for the general strain analysis. The diagram on the left represents the strains in the steel deck due to casting. Note the tensile strains at the top fibers and compressive strains at the bottom fibers of the steel deck cross section, representing the case for a single shore at centerline.

The second diagram in Fig. 20 represents strains due to shore removal, assuming that the force is applied to the composite section. The third diagram represents strains due to applied loading, and the fourth represents the superposition of the first three cases.

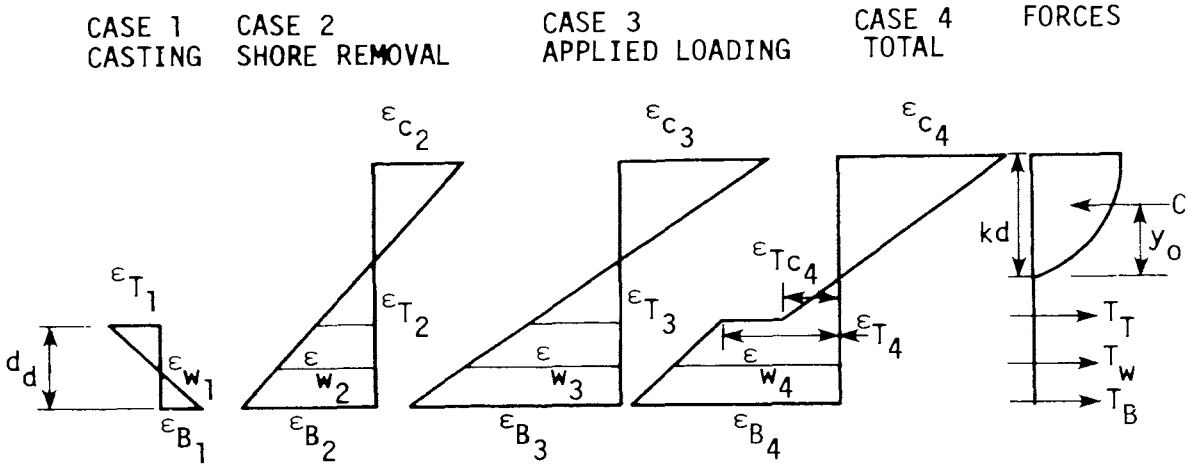

NOTE: TENSION STRAINS ARE PLOTTED TO THE LEFT AND COMPRESSION STRAINS ARE PLOTTED TO THE RIGHT.

Fig. 20. Strain-compatibility diagrams for general flexural strain analysis.

If one of the total strains, say the bottom strain of deck at rupture, is known, then the bottom strain for Case 3 can be calculated. The strain diagram for live loading (Case 3) is then found by interation to give the equilibrium of the internal compressive force and the tensile forces, i.e., until $C = T_T + T_W + T_B$. The compressive force, C, can be found from a theoretical stress-strain equation of the concrete; for example, such as that given by [10].

In order to complete the general strain flexural analysis, one quantity on the total strain diagram in Fig. 20 is needed; that one quantity could be any one of the strains indicated in the figure, i.e., ε_{C4}, ε_{T4}, ε_{W4}, or ε_{B4} or somewhere in between. For those decks having a steel stress-strain curve of small ductility, the controlling strain for the bottom fiber of deck (ε_{B4}) should be selected as the strain equal to 75% of that strain corresponding to the ultimate stress, if available, or, if not available, the designer may wish to use the strain corresponding to the yield stress. If enough ductility is capable of being developed, the controlling strain should be taken as $\varepsilon_{C4} = 0.003$ as limited by the ultimate strain of the concrete.

Other cases depend upon the definition of the design ultimate moment. For example, if the design is based upon initial yielding of the bottom fibers of deck, then ε_{B4} should be equal to the strain at the yield strength of the steel. Likewise, the design could be based upon the strain corresponding to that which causes buckling of the top fiber of deck, in which case ε_{T4} would be the controlling strain, or upon the maximum concrete compressive strain, ε_{C4}. If any criteria other than choosing ε_{B4} is used, then the strain determined for ε_{B4}

from the general analysis should be inspected to see if this strain development is possible as indicated by the steel coupon stress-strain relationship.

Several example results of the computations using the general strain analysis are contained in [11] (pp. 242-247). The examples are compared to the conventional ACI method shown by Equation (8). The examples show that a significant difference in computed ultimate moment capacity may result for the deeper deck cross sections.

Additional sample computational results in [11] indicate that, for the very high strength steel deck (F_y > 80 ksi), an unconservative moment capacity is determined if the (ACI) Equation (8) is used. This is due to the bottom fiber of deck reaching its rupture strength prior to the concrete reaching 0.003 strain. Thus, for a high strength steel deck the (ACI) Equation (8) is invalid, since the normal ductile beam behavior assumptions do not exist. Therefore, the examples in the above discussion indicate that the general strain analysis should be used for deck cross sections which do not develop yield stress across the entire deck section or for deck-reinforced elements which behave in a nonductile manner. However, additional experimental work is needed to more completely ascertain the correct flexural characteristics and the definition of failure.

7. DEFLECTION BEHAVIOR

Load-deflection behavior observed from the one-way slab element tests varied significantly depending primarily upon the shear span, span lengths, and steel deck thickness (stiffness of deck). An illustration of one type of load-displacement behavior which was associated with a shear-bond mode of failure is given in Fig. 21. The nominal dimensions of the member were 36 in. wide by 5.5 in. deep and 120 in. long, and the slab element contained an 18 gage steel deck section with a depth of 3 in. with embossments as a shear transferring device. The broken lines in Fig. 21 indicate calculated deflection relationships based upon the following moments of inertia, I: uncracked sections, effective according to ACI [7]; cracked sections; and an average of cracked and uncracked sections. Observations indicated that the simple average of cracked and uncracked moment of inertia sections provided a closer approximation to a conservative prediction of deflection nearer the expected working load range (assuming a factor of safety of about 1.8).

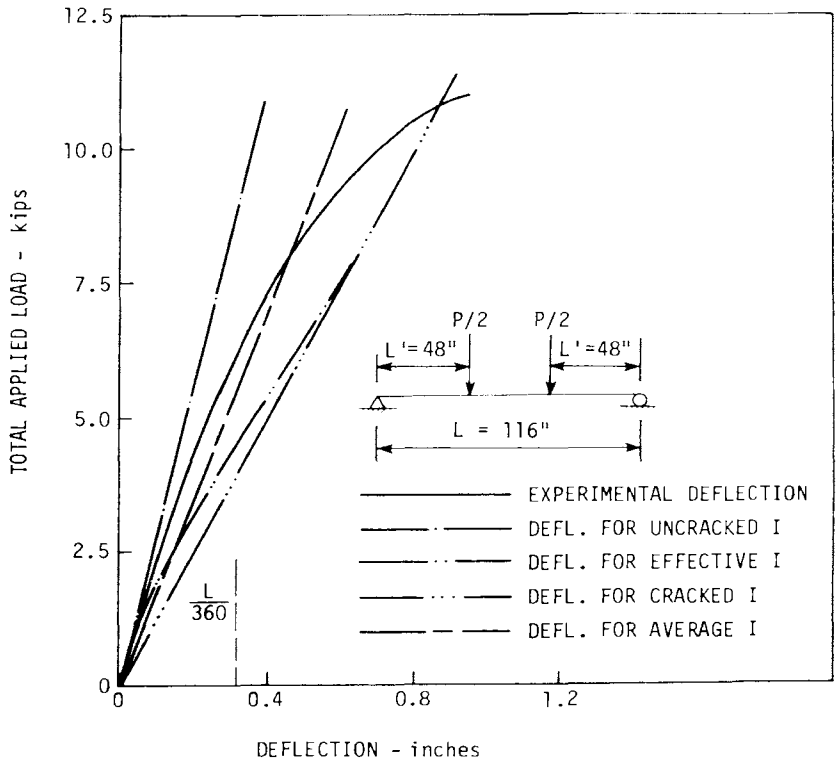

Fig. 21. Example of experimental vs theoretical load-deflection behavior.

8. REPEATED LOAD TESTS

As a means of gathering information on the basic fatigue characteristics of steel-deck-reinforced systems, 14 simply-supported slab elements consisting of two different steel deck sections were subjected to repeated loads. The fatigue tests were conducted with various load ranges and the resulting number of load cycles. The largest number of cycles applied was 2,800,000. These members characteristically exhibited shear-bond failures which were quite similar to failures obtained with specimens subjected to monotonic loading. The test results, in general, indicated favorable response characteristics and a relatively high load capacity for steel-deck-reinforced slab elements subjected to repeated loads. See [12] for further details.

9. CONTINUOUS SPANS

A preliminary investigation of the use of steel decking as reinforcement for continuous one-way slab elements was conducted with five specimens. Four of these had three spans as shown in Fig. 22 and one had two spans. Of the four three-span specimens (Fig. 22), two had conventional reinforcing bars as negative reinforcement over interior supports; also, two specimens each of 16- and 22-gage decks were tested. The basic load-deflection behavioral characteristics of the four three-span specimens are illustrated in Fig. 22. The ultimate failure of these continuous specimens was by shear-bond of the outside span in the region of the load point and the end reaction accompanied by the usual end-slip.

Analysis of a continuous span system is complicated by the aspect that the normal slippage failure associated with shear-bond of the interior spans is prevented by the blocking action of the outside adjacent spans. One possible solution is to separate the continuous system into equivalent simple beam segments in accordance with the inflection points determined from an indeterminate elastic analysis. The resulting equivalent span lengths are defined by L'' in Fig. 23. Thus, in effect, each beam segment subjected to positive bending with a length L'' is used for the shear-bond analysis. Additional tests and analyses are needed to provide more information for the shear-bond strength of interior spans of continuous systems.

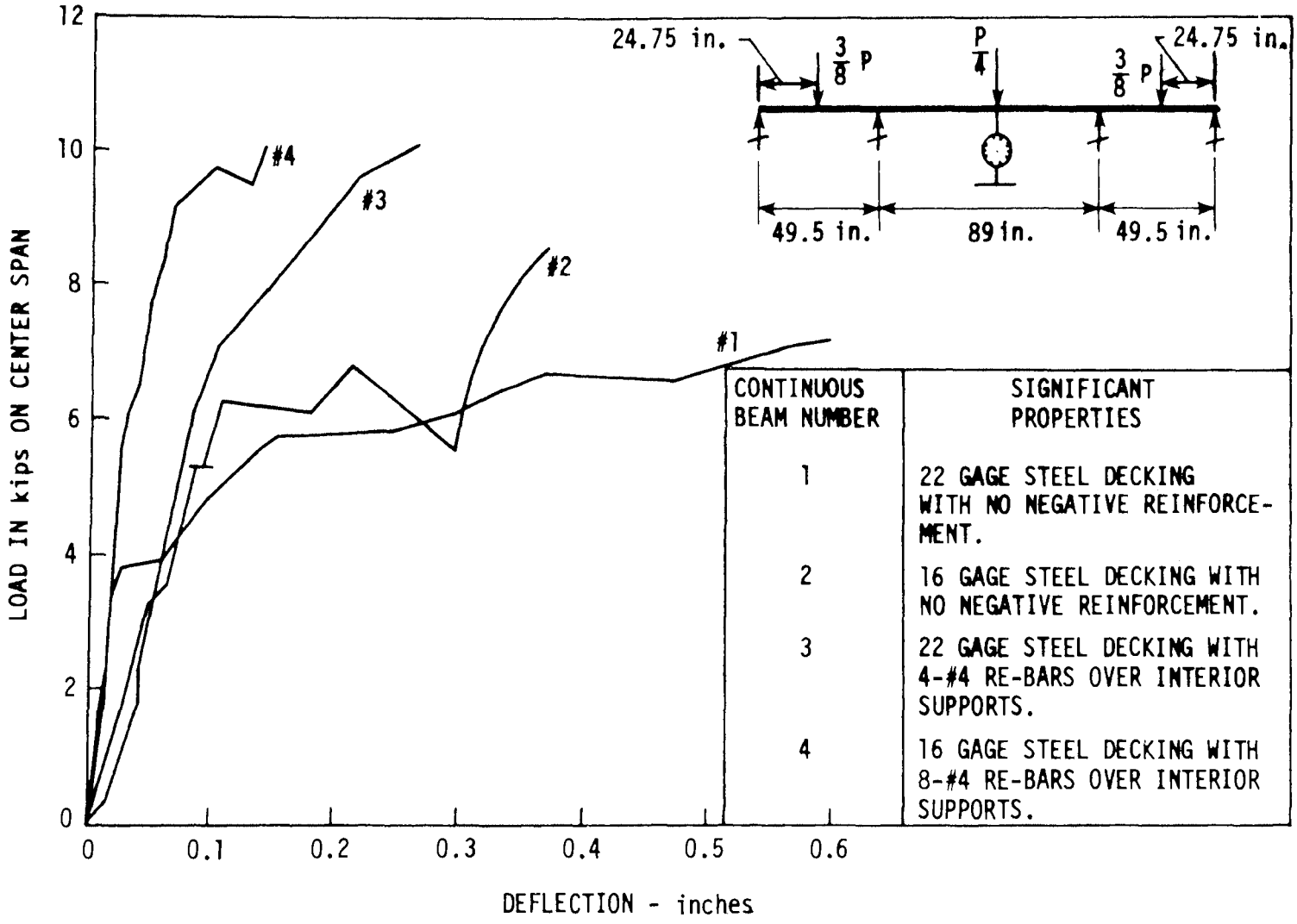

Fig. 22. Load vs centerline deflection of various continuous beams.

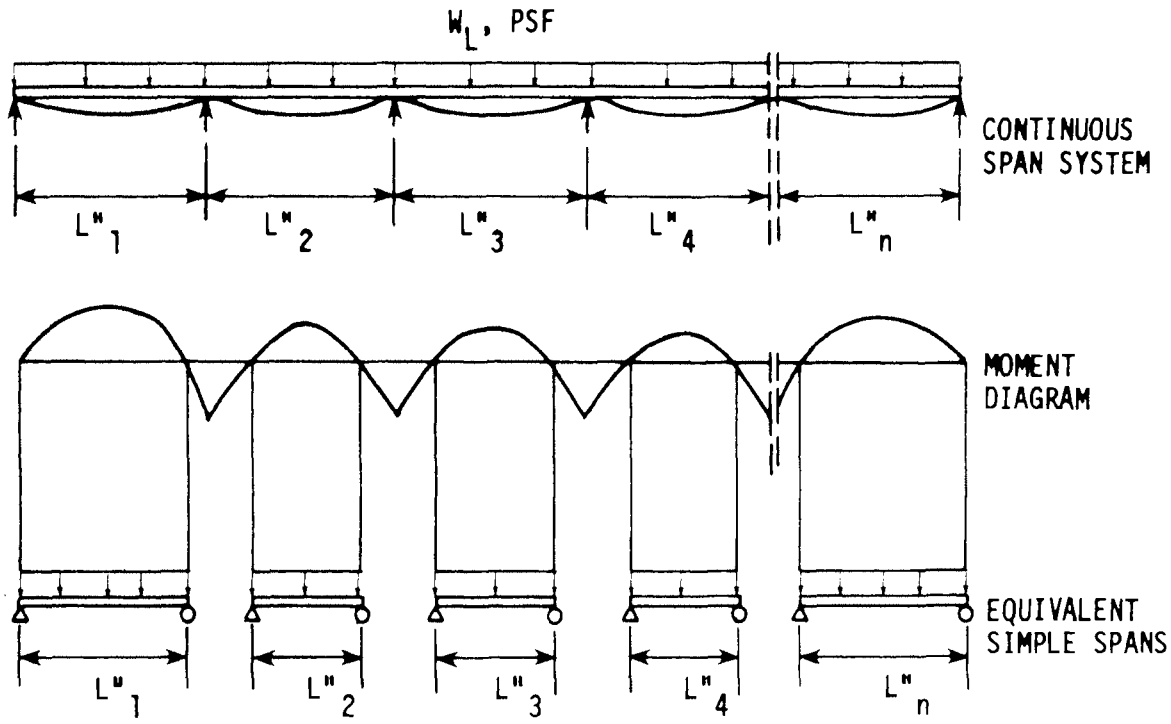

Fig. 23. Diagram showing how uniformly loaded continuous beam may be subdivided into a series of simple spans for analysis.

10. FULL-SCALE TWO-WAY SLABS

10.1 Description

An extensive investigation was undertaken to provide information which would be helpful for the design of steel deck slab systems subjected to concentrated loads [11]. Five full-scale slab panels having nominal dimensions of 16 ft by 12 ft by 4.5 or 5.5 in. were tested as shown in Fig. 24. The two-way slabs were simply supported along all four edges with the steel deck corrugations spanning the 12-foot dimension. The four concentrated loads were chosen to approximate a fork-lift truck type of loading.

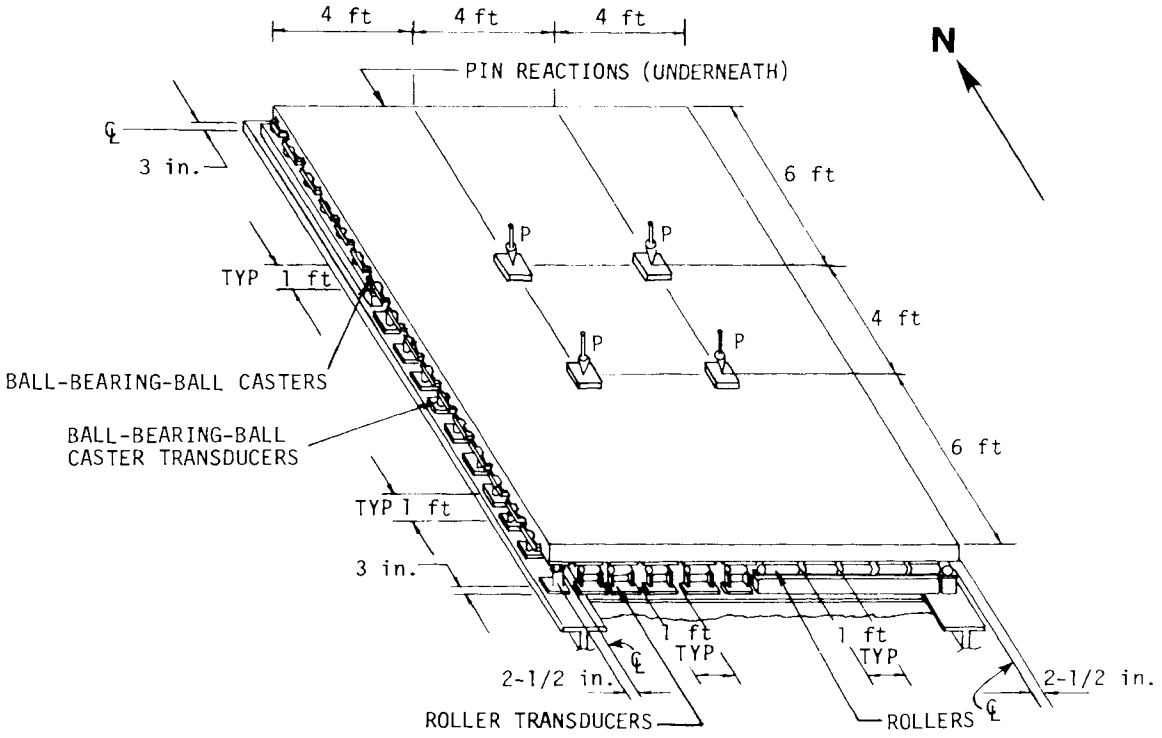

Fig. 24. General configuration and support conditions for full-scale slab tests.

The objectives of the two-way slab tests were the following.

1. Observe and investigate behavioral characteristics such as crack patterns, vertical deflections, reaction distributions, end-slip and concrete strains.

2. Determine the ultimate failure mode and load,

3. Determine the transverse distribution of concentrated loads, and

4. Develop an analysis based upon strength design concepts.

Each slab was subjected to the same mode of loading except that the first slab had all four corners restrained against vertical uplift. Each slab contained a different amount of supplementary reinforcement transverse to the deck corrugations. That is, Slab 1 contained 6 x 6 -6/6 (6x6 - W2.9xW2.9) welded wire fabric (WWF); Slab 2 contained 6 x 12 -0/4 (6x12 - W7xW4); and Slab 3 contained no supplementary reinforcing. Slab 4 contained No. 4 deformed wire spot welded traversing perpendicular to corrugations only, and Slab 5 contained 6 x 6 -10/10 (6x6 - W1.4x W1.4). Slabs 1, 2, and 4 had the supplementary reinforcement positioned directly on top of the steel deck, and Slab 5 had this reinforcement located approximately 1 in. down from the top surface of the concrete.

The five test slabs were composed of steel deck sections obtained from three different manufacturers. The first three slabs each contained the same type of embossed steel deck reinforcement having 20-gage steel with a depth of 1.55 in. Slab 4 contained a nominal 24-gage steel deck with a depth of 1.32 in. having transverse wires spaced at 3 in. intervals as shear transfer devices. Slab 5 contained an embossed deck of 20-gage steel having a depth of 3 in.

Table 6 provides a data summary of significant concrete and steel material properties for each slab. The tabulated cross-sectional areas and centroids of the steel deck are for a section perpendicular to the deck corrugations. Details concerning instrumentation and loading can be found in [11].

10.2. Test Results

Table 7 contains the applied ultimate and cycling loads for each of the five slabs. These tabulated loads are based on the amount of load applied at each of the four concentrated load points and include the weight of the loading apparatus, but they do not include the slab dead weight.

The test results in Table 7 indicate the value of supplementary reinforcing. Note that Slabs 2 and 4, containing the greater amount of

Table 6. Summary of significant material properties for two-way slab specimens.

Item	Slab 1	Slab 2	Slab 3	Slab 4	Slab 5
(a) Concrete					
Concrete compressive strength, f'_{ct}, in pounds per square inch	4,160	3,538	3,951	3,835	4,300
(b) Slab Thickness and Corner Support					
Average out-to-out thickness, in inches	4.83	4.62	4.62	4.68	5.44
Corner support condition	Restrained	Free	Free	Free	Free
(c) Steel Deck Properties					
Cross-sectional area, in square inches per foot	0.625	0.625	0.625	0.376	0.575
Deck depth, in inches	1.55	1.55	1.55	1.32	3.00
Steel thickness, in inches	0.0369	0.0369	0.0369	0.0252	0.0347
Centroid (from bottom) of steel cross section, in inches	0.63	0.63	0.63	0.665	1.504
Yield point or strength (at 0.5%), in kips per square inch	42.2	42.2	42.2	101.6	49.4
(d) Supplementary Reinforcing (WWF or Transverse Wires)					
Type	6x6-6/6	6x12-0/4	None	T-wires	6x6-10/10
Position	on deck	on deck	--	attached to deck	one inch from top of slab
Area parallel to deck corrugations, in square inches for foot	0.057	0.034	None	None	0.0282
Area transverse to deck corrugations, in square inches per foot	0.057	0.144	None	0.150	0.0282
Yield strength (at 0.5%) in kips per square inches	79.0	82.6 (No. 0 gage) 84.6 (No. 4 gage)	None	92.1	119.4

Table 7. Load results for five full-scale slab tests.

Parameter	Slab 1	Slab 2	Slab 3	Slab 4	Slab 5
Cycling load, in kips per load point	None	9.4	6.4	9.4	5.4
Ultimate load, P_u, in kips per load point	13.7	15.7	8.8	14.4	9.4
Equivalent ultimate uniform load, in pounds per square foot	305	345	196	321	209
Load at first observable end-slip, kips per load point	11.4	9.4	7.9	7.4	8.8
Percent of P_u for first end-slip	83	61	90	51	94

additional steel reinforcing transverse to the corrugations, sustained the higher ultimate loads. Thus, Slab 3, which had no supplementary reinforcing transverse to the corrugations, sustained the lowest ultimate load. Additional information concerning the effects of the supplementary reinforcing is contained in [11] and [14]. The ultimate load of Slab 1 would probably have been lower if subjected to the same conditions as Slabs 2 and 3. That is, Slab 1 was not cycled 10 times and had its corners restrained from uplift, thus allowing a somewhat higher ultimate load and an increased stiffness.

In conjunction with loads in Table 7, it is important to note the mode of failure associated with each slab. All five slabs failed ultimately by a shear-bond type of failure. This failure was characterized by a horizontal end slippage (along the east and west edges only) accompanied by diagonal edge cracks on the vertical faces over the central regions of the slabs. This end slippage was similar to that experienced in one-way slab element tests, except that the slab slippage only occurred along the central effective load-carrying part of slabs. No end slip was observed along the north and south edges.

None of the five slabs failed by extensive yielding of the steel deck. However, some limited yielding of the steel deck did occur in some load areas in the central regions or around the concentrated load points. None of the slabs failed by a concrete compressive type of failure. In addition, no punching shear failure occurred, although there were some signs of impending punching failure near the end of some of the tests.

The test results indicated an effective width somewhat greater than the distance between the concentrated loads. This behavior is shown in Fig. 25, which indicates the crack patterns for the first four slabs. The crack pattern for Slab 5 was similar to that of Slab 3. The numbers located beside each of the cracks indicate the order of occurrence. The effective width is approximated by L" in Fig. 25. The ultimate failure mode of all five slabs was that of shear-bond accompanied by end-slip over the central effective width region. An example of the end slip accompanied by diagonal edge cracking is shown by Slab 4 in Fig. 26.

The strength of the slabs was predicted by utilizing a shear-bond analysis in conjunction with the yield-line theory [13]. The crack patterns and corresponding effective widths verified the collapse mechanism as predicted by the yield-line approach. The collapse mechanism found to be valid for the five test slabs is shown in Fig. 27. The analysis procedure predicted the failure load for all slabs to within 9%. Details of this analysis procedure and the resulting design recommendations are contained in [11].

Behavior of the five slabs is clearly illustrated by the load-displacement relationship shown in Fig. 28. Slab 1 was subjected to monotonic loading from zero to ultimate, pausing only for instrumentation readings. The other four slabs were each cycled 10 times to an average cycling load of 64% of the ultimate load. The curves shown in Fig. 28 are for the final cycle to ultimate.

Figure 28 shows that Slab 2 not only carried the greatest load, but also sustained the highest ultimate deflection. This result can undoubtedly be attributed to the relatively large amount of supplementary steel. Slab 3, without any supplementary steel, indicated the least ultimate strength as well as the least ultimate deflection. In addition, all slabs except 3 and 5 exhibited fairly linear load-deflection relationships below the level defined by a deflection of L/180. Slabs 3 and 5 did show some nonlinear behavior at the L/180 level, and did not undergo as much ultimate deflection as did the other slabs. Vertical reaction force distributions were measured by the transducers indicated in Fig. 24. The resulting distribution of these forces is given in Fig. 29. The maximum error verified by summing all vertical load components was within 10% for Slabs 1, 2, 3, and 5. Slab 4 was omitted from Fig. 29, since its equilibrium force summation did not agree within 10%. The values shown at the extreme left along the west side of Slab 1 represent the average of the corner tie-down forces which were present only on Slab 1. The tie-down force is plotted as a negative value, since it acted downward, whereas the upward reactions were plotted as positive values. The other negative values in Fig. 29 occurred on the south side at a load just prior to ultimate and indicated a lifting off of the previously applied dead-load force; in fact,

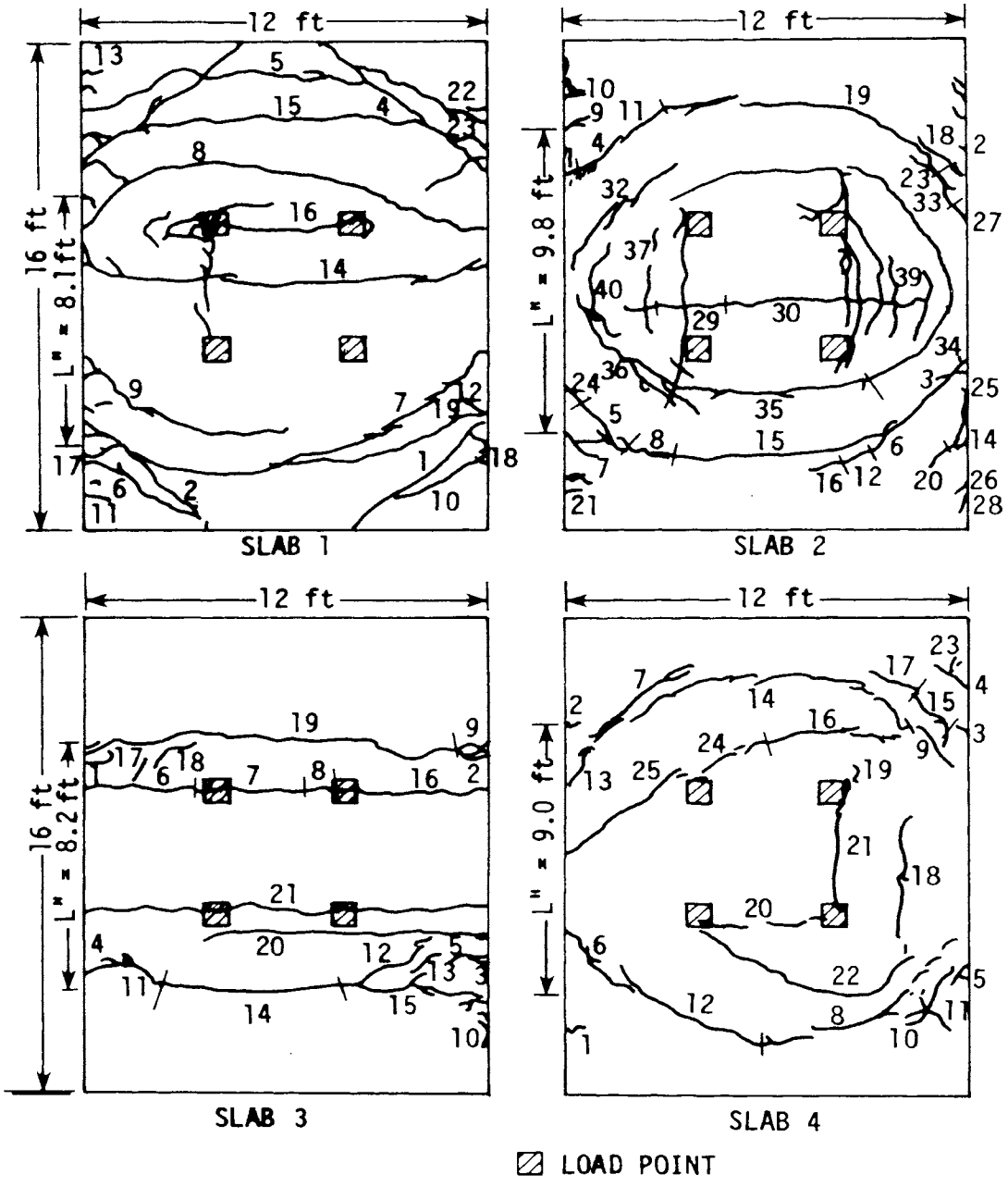

Fig. 25. Crack patterns on top surface of each slab.

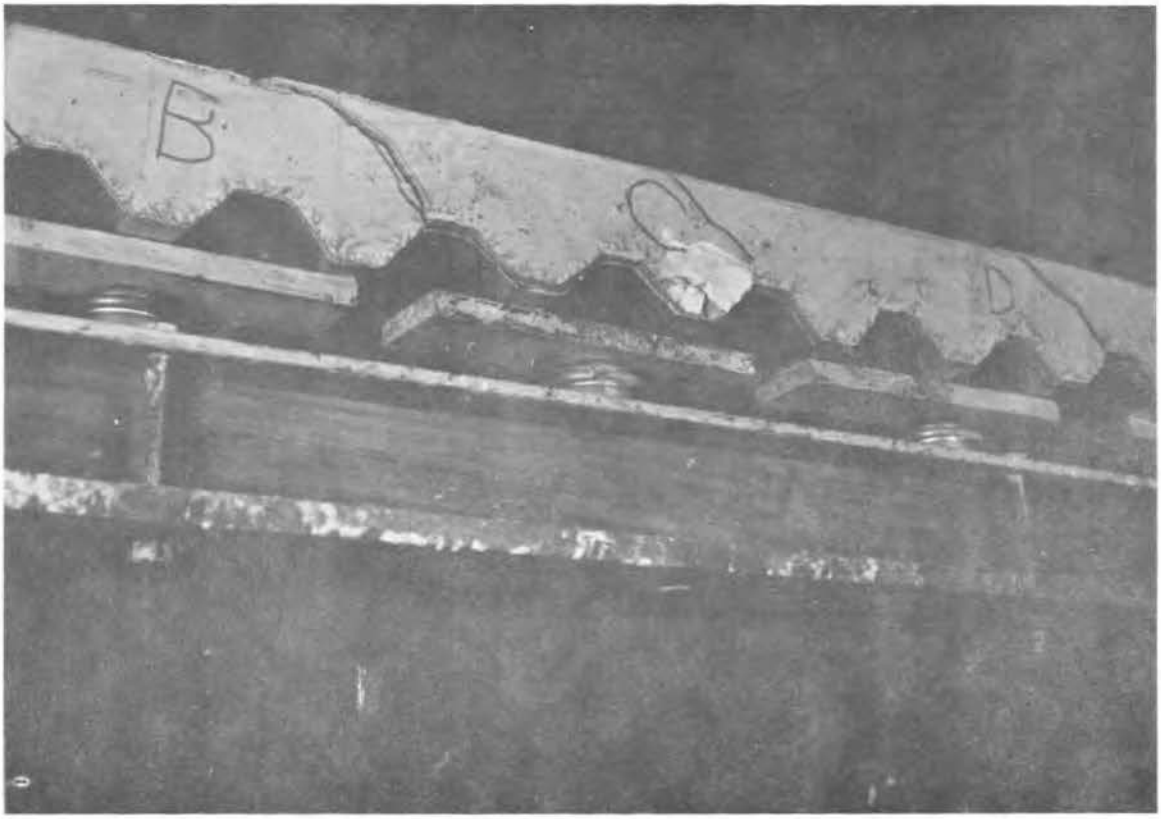

Fig. 26. View showing Slab 4 with diagonal edge cracking accompanied by end-slip.

Slab 3 completely lifted off its south support. The reaction distributions along the west side were generally trapezoidal in shape and correlated for the most part with the effective load-carrying segment of the slabs. The shape of the reaction distribution curves along the west edge became somewhat erratic after three-fourths of ultimate load due to the excessive cracking of the slabs.

The amount of total applied load distributed to each support beam along the west and south is shown in Fig. 30. Note that at commencement of load application, all slabs showed about 78% of the total applied load as transmitted to the west side in the so-called "strong" direction, except Slab 1, which indicated about 72% due to the corner tie-downs. Note that all slabs near ultimate had a west-edge-force summation of at least 97% of the total applied force. This result indicates that most of the force was carried in one-way action in the direction parallel to the corrugations. Additional behavioral characteristics can be found in [11], [15], and [16].

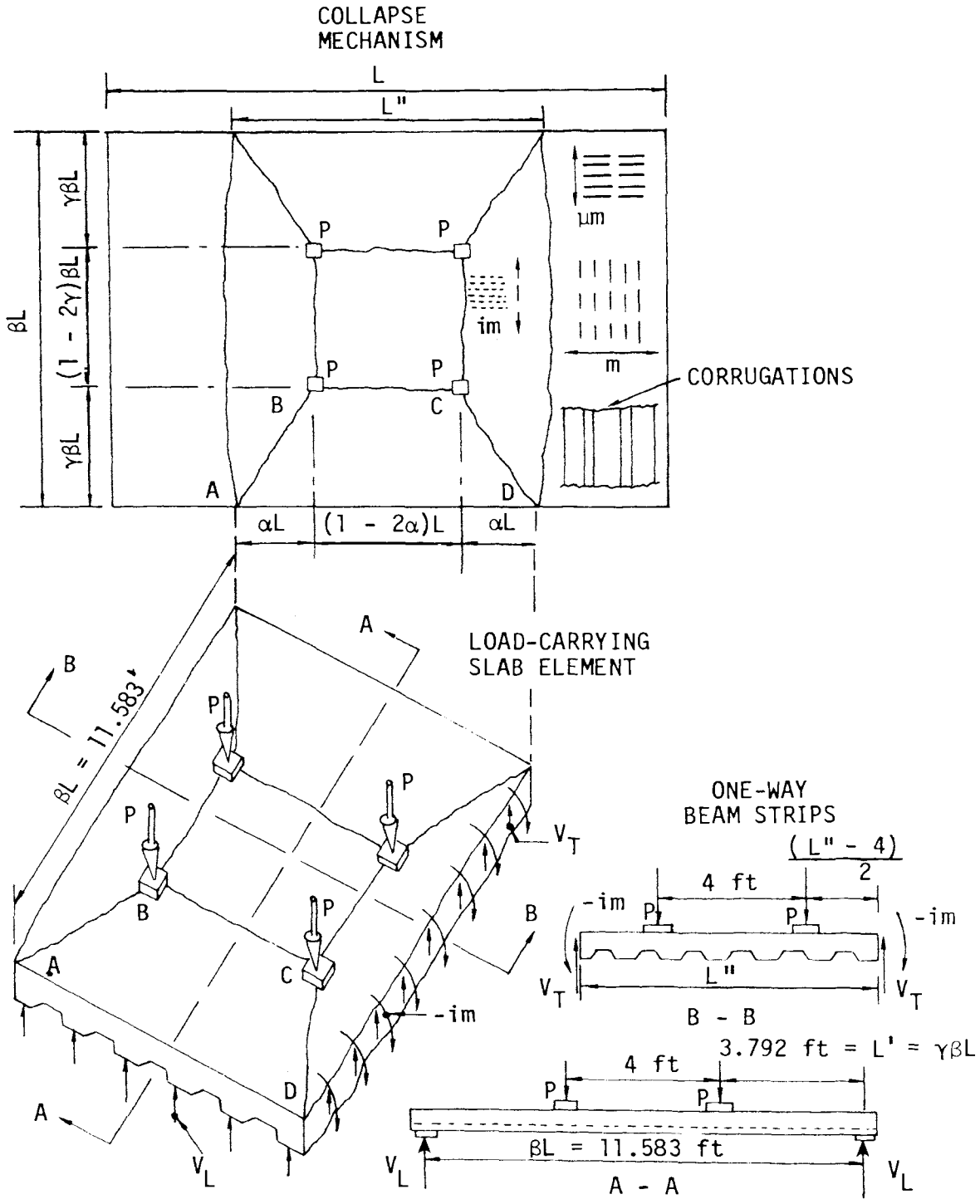

Fig. 27. Collapse mechanism and effective load-carrying segment used for analysis of five full-scale slabs.

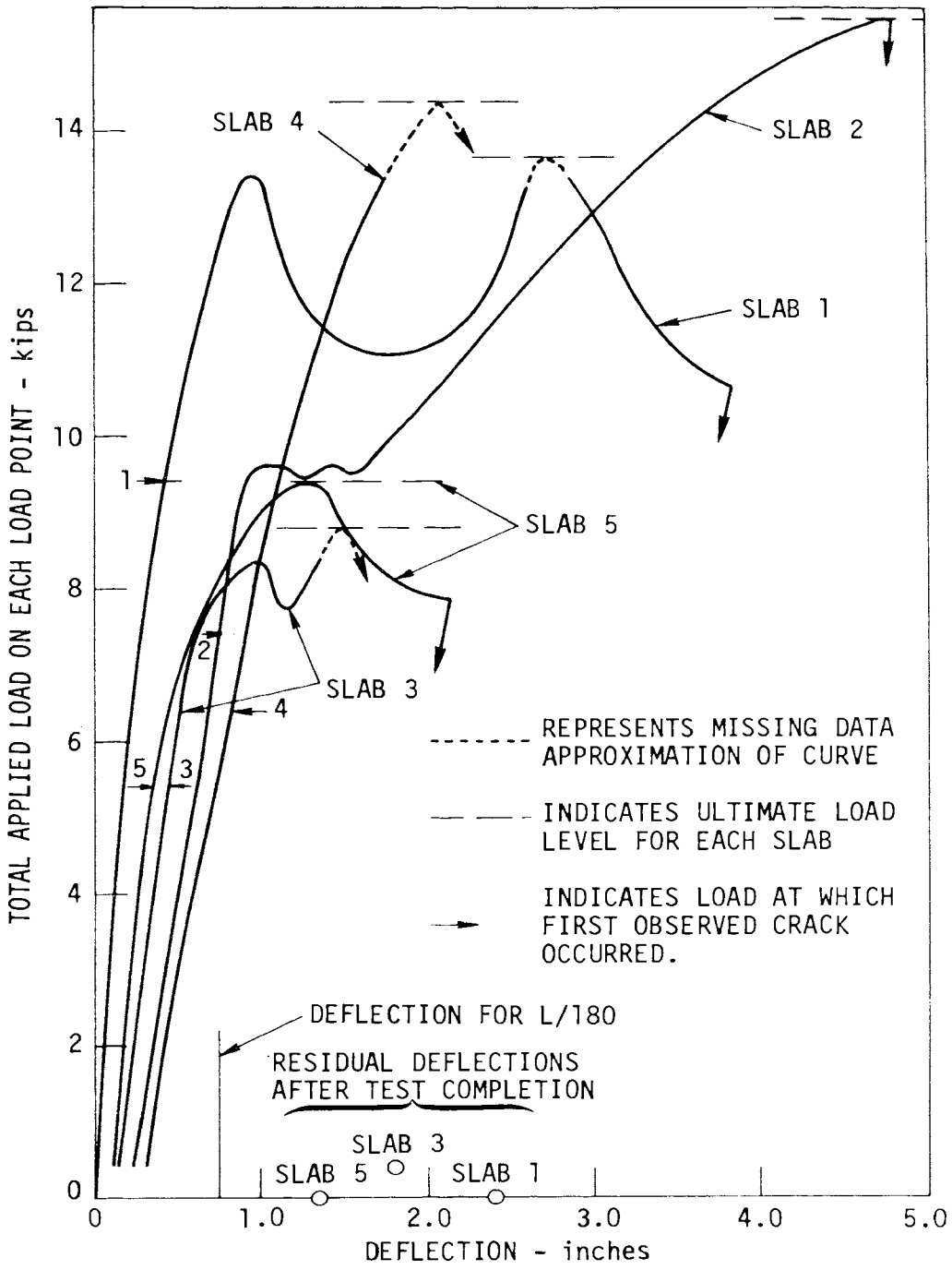

Fig. 28. Load vs centerpoint deflection for entire final load cycle.

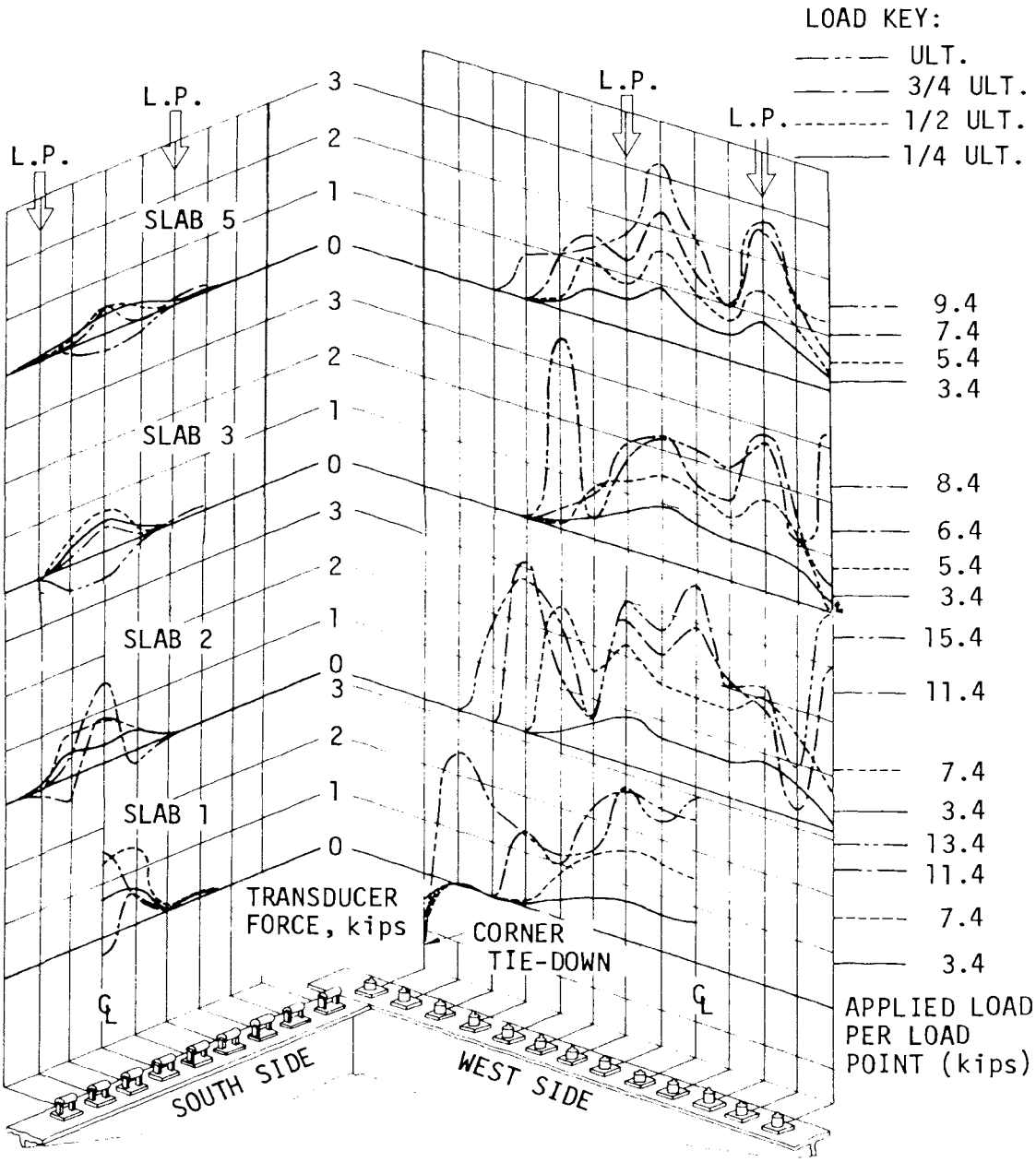

Fig. 29. Distribution of reactive forces along the south and west supports for Slabs 1, 2, 3, and 5.

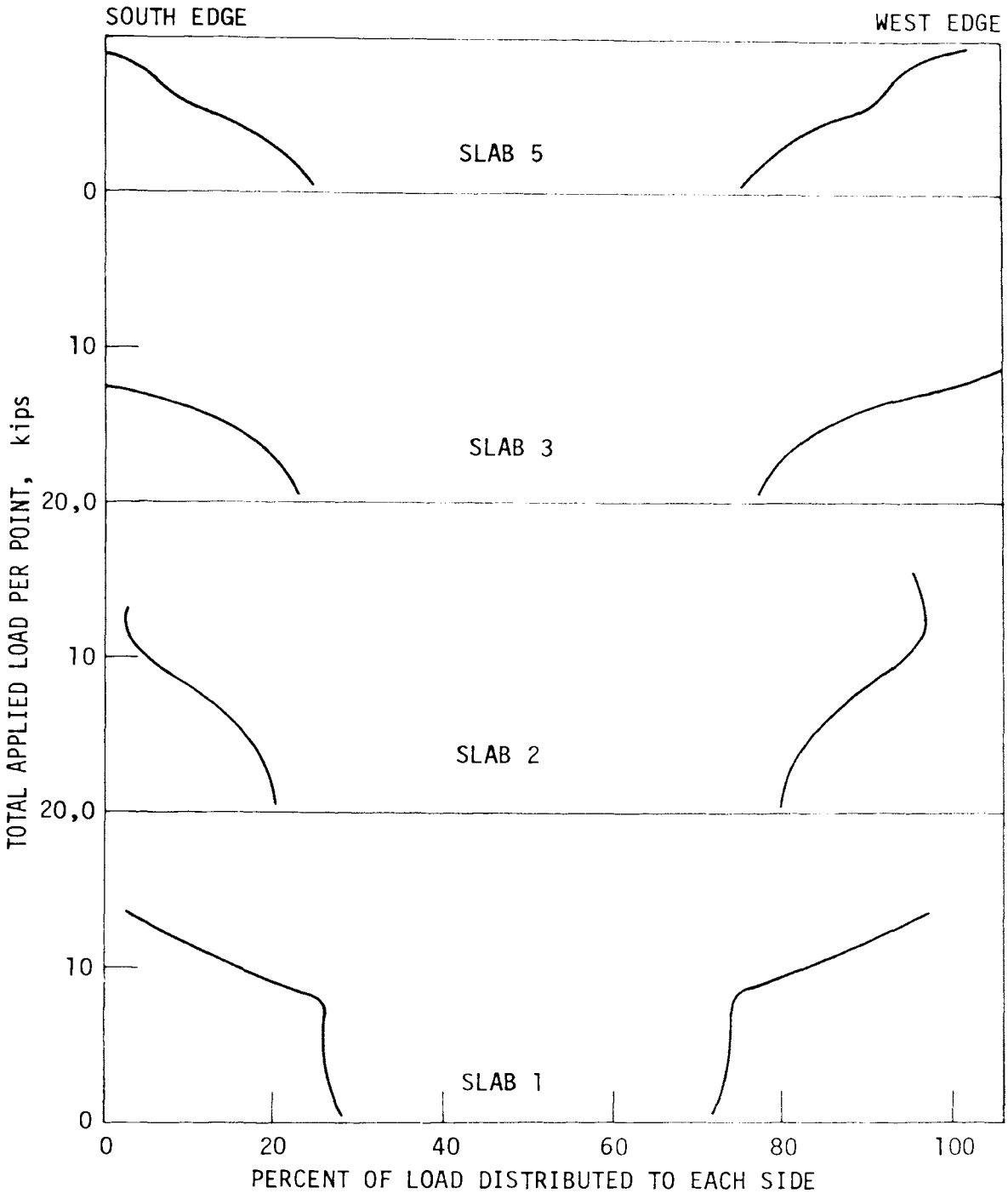

Fig. 30. Percentage of applied load transmitted to each reaction support as loading increases for Slabs 1, 2, 3, and 5.

11. ELEMENTS WITH TRANSVERSE CORRUGATIONS

Twelve slab elements were constructed with the steel deck corrugations perpendicular to the specimen and loaded as shown in Fig. 31. See [11].

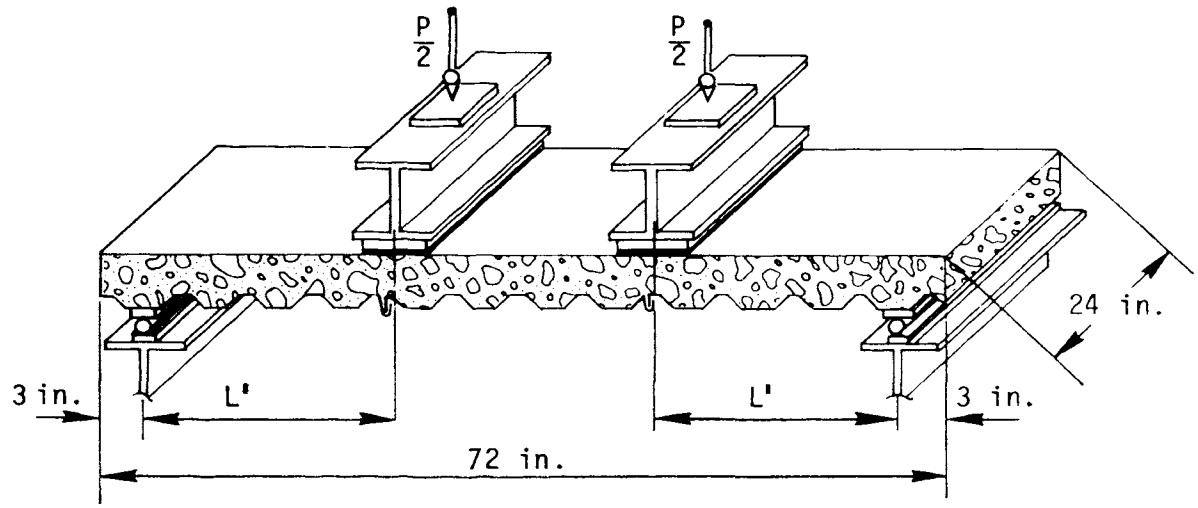

Fig. 31. Typical test on slab element with transverse decking.

The purpose of these tests was to determine the one-way strength transverse to the corrugations. The supplementary reinforcing was the same as contained in each of the five full-scale two-way slab tests. The results of the transverse tests were utilized to aid the analysis of the slabs.

Failure of those specimens containing no supplementary reinforcement was a sudden flexure collapse like that of a plain concrete beam, typically, a vertical crack appeared which extended upward from the corner of a corrugation near the center of the span. The moment capacity, M_u, of this section can be determined from the flexural strength of the concrete section above the deck, neglecting the steel deck cross section.

For those specimens containing supplementary reinforcement, the failure was characterized by yielding of the reinforcement. The added supplementary steel was placed directly on the deck, and resulted in a more ductile behavior. The failure was still characterized by a major flexural failure crack as described above. The ultimate flexural strength of sections containing supplementary reinforcement transverse

to the deck corrugations was found by a general strain analysis utilizing the usual ultimate strength computations, neglecting any beneficial effect of the presence of the steel decking [11]. These computations were based upon the assumption that the supplementary steel carries the tensile force and attains its yield strength.

12. EFFECTS OF VARIOUS SURFACE COATINGS

The effects of the type of surface coating were investigated with 34 one-way slab elements constructed with a constant, nominal depth, width, and length of 4.5 in., 24 in., and 144 in., respectively. Twenty-eight of these specimens were constructed with noncomposite decks (smooth decks), and six contained a composite deck utilizing embossments. Five different surface coatings were used on the cold-formed steel deck: plain deck (no surface coating), galvanized, enameled or painted, phosphatized or wiped, and rusted. Shear spans of 18, 36, and 54 in. were used. The purpose of the investigation was to ascertain behavior and strength characteristics due to the different surface coatings. Ultimate strength, deflections at ultimate load, strain energy absorbed and mode of failure were used as bases for comparison. A brief summary of the results, which are not yet available in published form, is given below.

The ultimate strength results indicated that the deck surface may be ranked in the following order from smallest to largest ultimate strength, galvanized, plain, enameled, wiped, enameled composite, galvanized composite, and rusted (all noncomposite unless otherwise stated).

The deflections at ultimate load provide an index as to the degree of warning prior to failure. The ranking, from smallest deflection to largest, is as follows: galvanized, plain, enameled, wiped, rusted, galvanized composite, and enameled composite.

Failure of all of these elements was via the shear-bond mode accompanied by end-slip. No end-slip was observed until failure for the slab elements constructed with smooth deck. However, end-slip was observed at both ends of the composite deck before failure. End-slip behavior indicated that the enameled composite deck was more favorable than the galvanized composite.

The ultimate strain energy stored in the slab elements provided a basis for comparing behavior under large loads. The ranking, according to increasing strain energy capacity, was galvanized, plain, enameled, wiped, rusted, galvanized composite, and enameled composite.

13. UNIFORM LOAD TESTS

To provide information as to the behavior of uniformly loaded specimens as compared with the previously tested concentrated load specimens, three nearly identical pairs of uniform versus concentrated load tests were performed on one-way slab elements. These six slab elements had nominal dimensions of 4.3 in. in depth by 24.2 in. in width by 8, 12, and 16 ft in length, respectively, for each pair of tests. The concentrated loads were applied as shown in Fig. 6 (with L' equal to one-fourth the span), whereas the uniform loads were applied by inflating a plastic bag which was confined between the top surface of the specimen and an inverted box. The test results have not yet been published; however, a brief description of behavioral characteristics is given below.

The failure mode for the uniform, as well as the concentrated load tests, was that of shear-bond accompanied by end-slip between the steel deck and concrete as typified in the previous one-way slab element tests. The major failure crack for the concentrated load tests was at or near the load point (at one-fourth of the span), while the major crack for the uniform load tests occurred near the 1/3 point of the span. The total ultimate load for the uniformly loaded specimens was observed to be from 3 to 19% more than the corresponding concentrated loaded specimens. The shear-bond regression analysis previously established for the one-way slab element tests indicated that this analysis also appears reasonably valid for the uniform tests. The replacement of the shear span, L', by an equivalent length of one-fourth of the span length for uniformly applied loads also appeared to be reasonably valid.

14. SLAB ELEMENTS WITH VARIOUS SHORING CONDITIONS

In actual construction practice, steel-deck-reinforced slabs are subjected to different shoring support conditions while the concrete is placed and cured. The two most common methods of support are at the ends only and at the ends and at midspan. In addition, several of the early ISU tests were supported continuously along the specimen's entire length. Thus, a question arises as to the effect in ultimate strength due to the various shoring conditions.

As a preliminary attempt to determine the effects of various shoring conditions, six nearly identical specimens were constructed having a nominal total depth of approximately 4 in., a width of 24.2 in., and a length of 10 ft. The six specimens were constructed in pairs subjected to the following three shore support conditions:

1. continuously supported along the entire length,
2. support at the ends and midspan, and
3. supported only near the ends.

The test results have not been completely published; however, a brief summary of the results is given below. See also published effects on shear-bond equation development in [5].

Test results of the six slab elements indicated that there was no significant difference between the six elements supported continuously and those supported at the ends and midspan. However, additional research needs to be performed for cases where the specimen dead load is a more significant portion of the total load-carrying capacity of the specimen. Due to the many variables affecting shear-bond strength, a complete determination of shoring condition effects on strength is quite complex. Results on shear-bond strength for separation of shoring conditions for all of the applicable 353 specimens tested at ISU were discussed in section 5.2.

15. SLAB ELEMENTS WITH VARIABLE AMOUNTS OF SUPPLEMENTARY REINFORCEMENT

As a preliminary attempt to ascertain the effect of the supplementary reinforcement, WWF, on shear-bond failure behavior, six specimens were cast. A comparison of the average results of each pair of identical specimens containing WWF to those containing no WWF is summarized below in Table 8. Since the area of supplementary steel was not appreciably different for four specimens containing WWF, an average of all four specimens containing WWF was compared to those not containing WWF. As can be seen in Table 8, the load capacity was apparently increased by 10.7%.

Table 8. Experimental effects of elements containing WWF.

Average of specimen	Area of WWF parallel to length, A_{s_1}, $(in.^2/ft)$	Average total applied load (kips)	Increase of lines 2 and 3 over line 1 (%)
2 and 4	0	10.3	--
1 and 5	0.039	11.35	10.7
3 and 6	0.057	11.45	

The influence on the shear-bond regression analysis can be observed by comparing these load values with the previously obtained shear-bond regression data. This is done in Fig. 32. The values shown were computed neglecting the area of WWF (which is small compared to deck area) in the computation of the reinforcement ratio, ρ. As can be seen, the slab element specimens containing WWF fall reasonably close to the previously plotted regression fit, but reflect about the same increase as shown in Table 8. Thus, the addition of the supplementary reinforcing did not appreciably affect the shear-bond strength by more than about 11%.

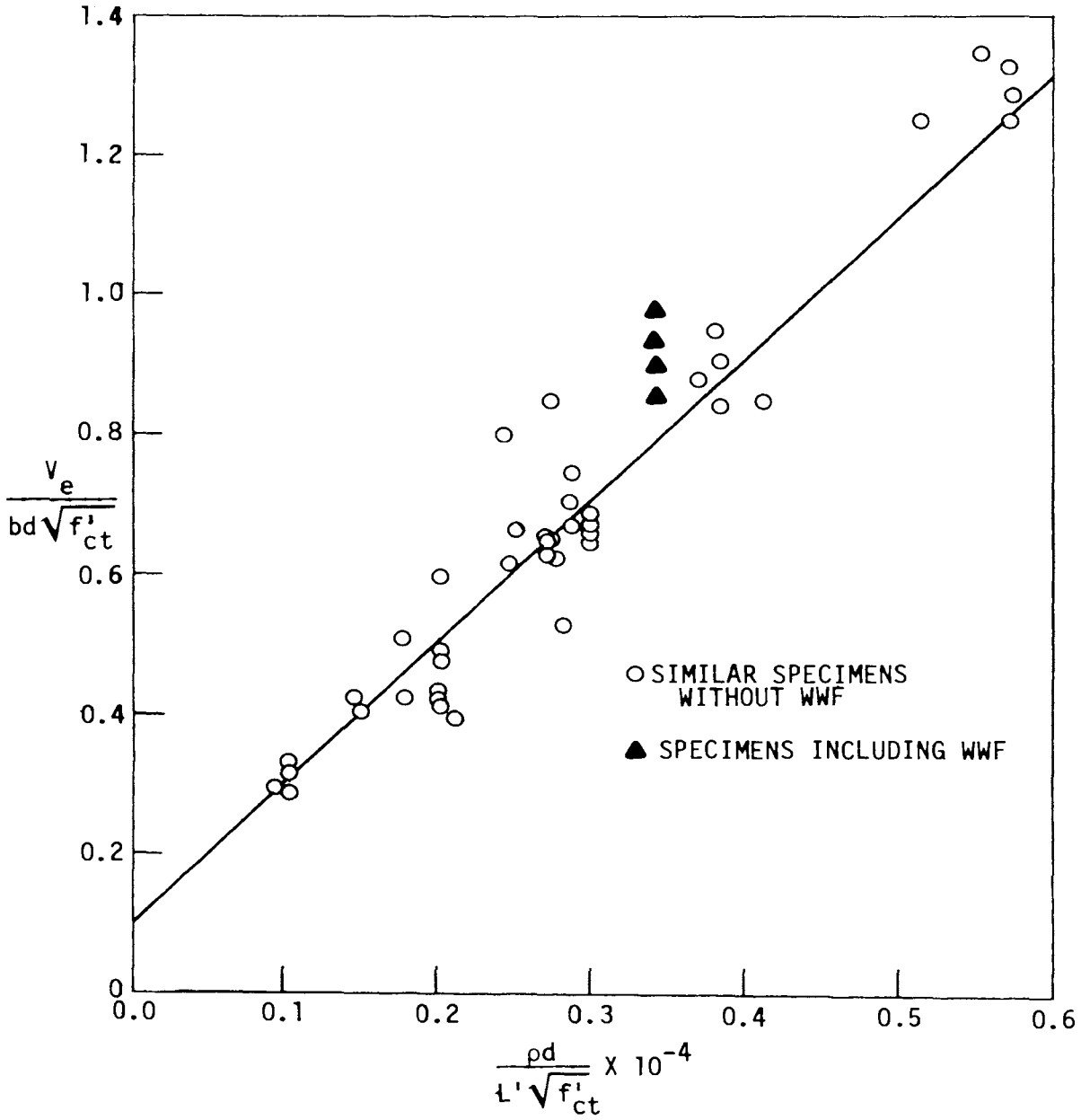

Fig. 32. Plot of shear-bond strength of slab elements containing WWF compared to those without WWF.

16. SUMMARY

A description of each type of test performed as part of an extensive experimental and theoretical research program conducted at Iowa State University has been presented. A total of 353 full-scale tests were conducted on the following types of specimens:

- pushout,
- single span slab elements with steel deck corrugations parallel to span length,
- slab elements with steel deck corrugations oriented transverse to span length,
- slab elements continuous over two or three spans,
- one-way elements subjected to repeated loading,
- slab elements constructed with variable supplementary reinforcement,
- one-way elements constructed with noncomposite deck with various surface coatings,
- full-size two-way floor slabs simply supported on four edges,
- slab elements with various shoring conditions, and
- one-way elements subjected to uniform versus concentrated loading.

In addition, 151 one-way elements tested by steel deck manufacturers were included in the investigation.

The modes of failure are shear-bond and flexure of an over- and under-reinforced section. The predominant mode of failure for steel-deck-reinforced slab systems is that of shear-bond accompanied by end-slip resulting from a horizontal slippage between the steel and concrete.

Equations based upon a regression analysis were formulated for the shear-bond capacity of steel-deck-reinforced slab systems, and design recommendations were published [4]. The American Society of Civil Engineer's Technical Council on Codes and Standards Committee on Composite Steel Deck Slabs is currently utilizing pertinent information gained from this investigation to develop standards for possible adoption by the design profession.

17. REFERENCES

1. Porter, M. L., L. W. Timm, and C. E. Ekberg, Jr., "Compilation of Test Data Pertaining to One-Way Concrete Slab Elements Reinforced with Cold-Formed Steel Decking," Iowa State University Engineering Research Institute Report, ISU-ERI-AMES-74086, Ames, Iowa, May 1974.

2. Porter, M. L., L. W. Timm, and C. E. Ekberg, Jr., "Manufacturer's Test Data of One-Way Concrete Slab Elements Reinforced with Cold-Formed Steel Decking," Iowa State University Engineering Research Institute Report, ISU-ERI-AMES-74109, Ames, Iowa, June 1974.

3. Porter, M. L., "Investigation of Light Gage Steel Forms as Reinforcement for Concrete Slabs," unpublished MS Thesis, Iowa State University, Ames, Iowa, 1968.

4. Porter, M. L., C. E. Ekberg, Jr., "Design Recommendations for Steel Deck Floor Slabs," Journal of the Structural Division, Proceedings of the American Society of Civil Engineers, Vol. 102, No. ST11, Paper 12528, November, pp. 2121-2136, 1976.

5. Porter, M. L., C. E. Ekberg, Jr., L. F. Greimann, and H. A. Elleby, "Shear-Bond Analysis of Steel-Deck-Reinforced Slabs," Journal of the Structural Division, Proceedings of the American Society of Civil Engineers, Vol. 102, No. ST12, Paper 12611, December, pp. 2255-2268, 1976.

6. Schuster, R. M., "Strength and Behavior of Cold-Rolled Steel-Deck Reinforced Concrete Floor Slabs," unpublished Ph.D. Thesis, Iowa State University, Ames, Iowa, 1970.

7. American Concrete Institute, "Building Code Requirements for Reinforced Concrete" (ACI 318-77), and Commentary thereon, as published by the American Concrete Institute, Box 19150, Detroit, Michigan, 1977.

8. Zsutty, T. C., "Beam Shear Strength Prediction by Analysis of Existing Data," Proceedings, Journal of the American Concrete Institute, 65(11):943-951, November 1968.

9. American Iron and Steel Institute, "Specification for the Design of Cold-Formed Steel Structural Members," and Commentary thereon, Committee on Building Research and Technology, American Iron and Steel Institute, Washington, D.C., 1968 edition with Addendum No. 1, 7th printing, 1977.

10. Smith, G. M., and L. E. Young, "Ultimate Flexural Analysis Based on Stress-Strain Curves of Cylinders," Proceedings, Journal of the American Concrete Institute, 28(6):597-609, December 1956.

11. Porter, M. L., "The Behavior and Analysis of Two-Way Simply Supported Concrete Floor Slabs Constructed with Cold-Formed Steel Decking," unpublished Ph.D. Thesis, Iowa State University, Ames, Iowa, 1974.

12. Mouw, K. W. and C. E. Ekberg, Jr., "Fatigue Testing of Light Gage Metal Forms," Engineering Research Institute, Special Report, ERI-348, Iowa State University, Ames, Iowa, 1969.

13. Jones, L. L., and R. H. Wood, Yield-Line Analysis of Slabs, American Elsevier Publishing Company, Inc., New York, 1967.

14. Porter, M. L., "Effects of Added Reinforcement in Steel-Deck Slabs," Fourth International Specialty Conference on Cold-Formed Steel Structures, St. Louis, Mo., June, pp. 837-870, 1978.

15. Porter, M. L. and C. E. Ekberg, Jr., "Summary of Full-Scale Laboratory Tests of Concrete Slabs Reinforced with Cold-Formed Steel Decking," Ninth Congress of the International Association for Bridge and Structural Engineering, Preliminary Report, Zurich, pp. 173-183, 1972.

16. Porter, M. L., C. E. Ekberg, Jr., "Behavior of Steel-Deck-Reinforced Slabs," Journal of the Structural Division, Proceedings of the American Society of Civil Engineers, Paper 12826, Vol. 103, No. ST3, March, pp. 663-677, 1977.

18. APPENDIX: COMPLETE LIST OF PUBLISHED PAPERS AND THESES RELATING TO ISU RESEARCH

1. Ekberg, C. E., Jr., and Schuster, R. M., "Floor Systems with Composite Form-Reinforced Concrete Slabs," Eighth Congress of the International Association for Bridge and Structural Engineering, Final Report, Zurich, pp. 385-394, 1968.

2. Porter, M. L., "Investigation of Light Gage Steel Forms as Reinforcement for Concrete Slabs," MS Thesis, Iowa State University, Ames, Iowa, 1968.

3. Schuster, R. M., "Strength and Behavior of Cold-Rolled Steel-Deck-Reinforced Concrete Floor Slabs," Ph.D. Thesis, Iowa State University, Ames, Iowa, 1970.

4. Porter, M. L. and Ekberg, C. E., Jr., "Investigation of Cold-Formed Steel-Deck-Reinforced Concrete Floor Slabs," Proceedings of First Specialty Conference on Cold-Formed Steel Structures, Dept. of Civil Engineering, University of Missouri-Rolla, pp. 179-185, August 19-20, 1971.

5. Porter, M. L. and Ekberg, C. E., Jr., "Summary of Full-Scale Laboratory Tests of Concrete Slabs Reinforced with Cold-Formed Steel Decking," Ninth Congress of the International Association for Bridge and Structural Engineering, Preliminary Report, Zurich, pp. 173-183, 1972.

6. Schuster, R. M., "Composite Steel-Deck-Reinforced Concrete Systems Failing in Shear-Bond," Ninth Congress of the International Association for Bridge and Structural Engineering, Preliminary Report, Zurich, pp. 185-191, 1972.

7. Porter, M. L., "The Behavior and Analysis of Two-Way Simply Supported Concrete Floor Slabs Constructed with Cold-Formed Steel Decking," Ph.D. Thesis, Iowa State University, Ames, Iowa, 1974.

8. Porter, M. L., "Commentary on the Tentative Recommendations for the Design of Composite Steel Deck Slabs," Manual written for American Iron and Steel Institute, Washington, D.C., December 1974.

9. Porter, M. L. and Ekberg, C. E., Jr., Discussion of paper by the Subcommittee on the State-of-the-Art Survey of the Task Committee on Composite Construction of the Committee on Metals of the Structural Division entitled "Composite Steel-Concrete Construction," ASCE Journal of the Structural Division, Vol. 101, No. ST3, pp. 615-616, March 1975.

10. Porter, M. L. and Ekberg, C. E., Jr., "Tentative Design Recommendations for Steel Deck Reinforced Floor Slabs," Proceedings of Third Specialty Conference on Cold-Formed Steel Structures, Dept. of Civil Engineering, University of Missouri-Rolla, pp. 761-792, October 1975.

11. Porter, M. L. and Ekberg, C. E., Jr., "Design vs Test Results for Steel Deck Floor Slabs," Proceedings of Third Specialty Conference on Cold-Formed Steel Structures, Dept. of Civil Engineering, University of Missouri-Rolla, pp. 793-812, October 1975.

12. Porter, M. L., Ekberg, C. E., Jr., Greimann, L. F., and Elleby, H. A., "Shear-Bond Analysis of Steel-Deck-Reinforced Slabs," Journal of the Structural Division, Proceedings of the American Society of Civil Engineering, Paper 12611, Vol. 102, No. ST12, pp. 2255-2268, December 1976.

13. Porter, M. L., Ekberg, C. E., Jr., "Design Recommendations for Steel Deck Floor Slabs," Journal of the Structural Division, Proceedings of the American Society of Civil Engineering, Paper 12528, Vol. 102, No. ST11, pp. 2121-2136, November 1976.

14. Porter, M. L., Ekberg, C. E., Jr., "Behavior of Steel-Deck Reinforced Slabs," Journal of the Structural Division, Proceedings of the American Society of Civil Engineers, Paper 12826, Vol. 103, No. ST3, pp. 663-677, March 1977.

15. Porter, M. L., Discussion of paper "Composite Steel-Deck Concrete Floor Systems," by Reinhold M. Schuster, Discussion paper published in Journal of the Structural Division, Proceedings of the American Society of Civil Engineers, pp. 926-927, April 1977.

16. Porter, M. L., "Effects of Added Reinforcement in Steel-Deck Slabs," Fourth International Specialty Conference on Cold-Formed Steel Structures, St. Louis, Mo., pp. 837-870, June 1978.